A two-process model of *Drosophila* sleep reveals an inter-dependence between circadian clock speed and the rate of sleep pressure decay

Lakshman Abhilash, Orie Thomas Shafer[#]

The Advanced Science Research Center, The City University of New York; The Graduate Center at the City University of New York

Running title: Drosophila two-process model

[#]Correspondence: oshafer@gc.cuny.edu

Abstract

Sleep is controlled by two processes – a circadian clock that regulates its timing and a homeostat that regulates the drive to sleep. *Drosophila* has been an insightful model for understanding both processes. For four decades, Borbély and Daan's two-process model has provided a powerful framework for understanding how circadian and homeostatic processes regulate sleep. However, the field of fly sleep has not employed such a model as a framework for the investigation of sleep. To this end, we have adapted the two-process model to the fly and establish its utility by showing that it can provide empirically testable predictions regarding the circadian and homeostatic control of fly sleep. We show that the ultradian rhythms previously reported for loss-of-function clock mutants are a predictable consequence of a functional sleep homeostat in the absence of a functioning circadian system. We find that a model in which the circadian clock speed and homeostatic rates act without influencing each other provides imprecise predictions regarding how clock speed influences the strength of sleep rhythms and the amount of daily sleep. We also find that quantitatively good fits between empirical values and model predictions were achieved only when clock speeds were positively correlated with rates of decay of sleep pressure. Our results indicate that longer sleep bouts better reflect the homeostatic process than the current definition of sleep as any inactivity lasting five minutes or more. This two-process model represents a powerful framework for future work on the molecular and physiological regulation of fly sleep.

Keywords: Drosophila, sleep, circadian, sleep homeostat, two-process model, free-running, period, ultradian rhythms

Introduction

Sleep-like states are ubiquitous within the animal kingdom [1] and the complexity of sleep behavior has prompted many attempts to mathematically model its regulation. Such models provide a powerful quantitative framework for the experimental investigation of sleep regulation across taxa. They are particularly useful by virtue of their provision of testable hypotheses [2–9]. Among the most successful models of sleep regulation are variants of Borbély's two-process model [2,4–7], which posits the presence of a sleep pressure that builds during wakefulness (Fig. 1A). Once this sleep pressure reaches an upper threshold, sleep is induced. During sleep, pressure falls until it reaches a lower threshold, at which point wakefulness is initiated. According to this model, the build-up and discharge of sleep pressure is driven by one process – the sleep homeostatic component or the S-process, whereas the upper and lower thresholds change predictably throughout the day and are set by a second process– the circadian clock or the C-process (Fig. 1A). Though myriad factors impact sleep [10], the regulation of typical sleep/wake cycles can be explained by just these two processes acting in concert but operating separately, that is, the S-process can operate without a functional C-process and *vice versa* [6,7].

The two-process model has provided a powerful conceptual framework in the field for nearly four decades owing to its ability to explain changes in slow wave sleep and predict the timing and amount of sleep, particularly in humans, both during normal sleep/wake cycles and in the aftermath of sleep deprivation [5–7]. The model has also been used over the years to inform sleep clinicians in the treatment of sleep disorders associated with major depression, seasonal affective disorders, irregular sleep patterns, and the application of bright light therapy [7]. Additionally, the model provides a powerful, quantitative framework for assessing interactions between the two processes

67 and how they might contribute to the control of sleep [11]. Despite the longstanding utility of the
68 two-process model for understanding human sleep, it has been underutilized as a quantitative
69 platform for understanding the regulation of sleep in model systems amenable to the genetic and
70 molecular manipulation of the brain.
71
72 Though *Drosophila* has been a critical model system for understanding the genetic, neuronal and
73 physiological bases of circadian rhythms since the 1970s, it has become an informative model for
74 understanding sleep only over the past two decades [12–14]. Furthermore, because of the
75 availability of a powerful array of genetic tools and the ability to regulate gene expression spatially
76 and temporally in the fly, the *Drosophila* sleep field has made significant advances in
77 understanding the regulation of sleep [15–17]. While much of the focus of fly sleep research has
78 been on the identification of genes and neural networks that regulate the amount of sleep
79 [14,16,18–27] relatively little is known about the regulation of sleep timing (e.g., [28]). Therefore,
80 much remains to be learned about how circadian clocks and homeostatic control mechanisms
81 interact to regulate multiple aspects of sleep.
82
83 While there are significant gaps in our understanding of sleep regulation, the fly continues to
84 provide insights into its mechanisms [14]. A major reason for this is the apparent similarity
85 (behavioral, genetic, and physiological) between fly and mammalian sleep [29]. For example, as
86 in mammals, flies display bouts of extended inactivity characterized by increased arousal
87 thresholds, rapid reversibility, and homeostatic rebound in response to sleep deprivation
88 [12,15,30]. In addition, a major feature of mammalian sleep is the occurrence of distinct stages of
89 sleep, i.e., rapid eye movement (REM) and several non-REM (NREM) sleep stages [31]. Although

90 various durations of inactivity have previously been classified as distinct epochs of sleep [12,32],
91 fly sleep is now almost universally treated as a unitary state, with any period of inactivity lasting
92 more than five minutes being considered a sleep like state [14,32]. However, recent work has
93 provided strong evidence for multiple sleep stages in flies, with longer bouts of inactivity
94 representing physiologically, metabolically, and behaviorally distinct sleep states compared to
95 shorter bouts [33–39], thereby adding an additional degree of similarity in sleep between flies and
96 mammals.
97
98 Owing to the predictive power of the two-process model of human sleep regulation, we sought to
99 establish a quantitative theoretical framework for a two-process model of fly sleep. Here we
100 describe the adaptation of such a model, identify the sleep homeostatic parameters that best explain
101 fly sleep, and use it to reveal interesting relationships between sleep and the circadian clock and
102 highlight the utility of this quantitative model in understanding fly sleep. Based on this work, we
103 also propose that longer durations of inactivity, which have been recognized by others as reflecting
104 a relatively deep sleep state, are likely a stronger reflection of sleep homeostatic processes in
105 *Drosophila* than the currently employed unitary definition of fly sleep as any bout of inactivity
106 lasting five minutes or more.
107

108 # Results

109 **Circadian time-series analysis of *Drosophila* sleep**

110 Though sleep is considered a major output of the circadian system, sleep behavior in flies has
111 rarely been subjected to circadian time-series analysis. The vast majority of studies use locomotor
112 activity, typically measured as infrared beam crossings, for such analyses. However, to fully
113 understand the circadian control of sleep, time-series analyses should be performed directly on
114 sleep data. For this reason, we have developed an analysis package [40], which is now available
115 on the Comprehensive R Archive Network (CRAN; https://cran.r-
116 project.org/web/packages/phase/index.html). Like double plotted actograms for locomotor
117 activity, sleep rhythms can be visualized as double plotted "somnograms" (Fig. 1B). Consistent
118 with previous work [12,14,30], somnograms reveal two distinct phases of increased sleep under
119 light/dark (LD) cycles, one during the daytime and one during the nighttime (Fig. 1B). Although
120 the field has long recognized that fly sleep is bimodal, in that there are two major episodes of sleep
121 in each diurnal or circadian cycle [12,14,30], traditional time-series methods to quantitatively
122 assess bimodality and periodicity in sleep time-series have not been employed. We used the Chi-
123 squared (χ^2) periodogram [41] on sleep time-series data to analyze the two daily peaks of sleep
124 under both LD cycles and constant darkness (DD), revealing two clear peaks in the periodogram,
125 one at 12-h and the other at 24-h (Fig. 1C). Though largely similar, there are subtle differences
126 between the periodograms of sleep and activity data measured under LD cycles and DD (Figs. 1C
127 and 1D, compare across panels and see Table 1). The powers of average sleep time-series are
128 higher than the powers of locomotor activity time-series (see Table 1). This is not a mere
129 consequence of using the Chi-square periodogram, whose limitations for the quantitative

130 assessment of rhythmic power has been described [42–44], as similar results were also obtained
131 using the Lomb-Scargle periodogram (Suppl. Table 1).
132
133 Using the Chi-square periodogram, the 12-h peak is typically lower than the 24-h peak in
134 periodograms, but this difference is much smaller for the locomotor activity periodograms
135 compared to sleep periodograms – in other words, the 12- and 24-h periodogram peaks are of more
136 comparable height for locomotor activity (compare Figs. 1C and 1D). Therefore, we emphasize
137 that irrespective of the periodogram method used, it is critical to employ sleep data to perform
138 long-term time-series analyses rather than using locomotor activity, if one is to address the
139 circadian regulation of sleep directly. Next, using the last four cycles under entrainment, we
140 estimated the percentage of a 24-h day that a fly spends sleeping. Across the three genotypes, we
141 found that flies spend ~70 to 80% of their day sleeping (Fig. 1E). We used these two general
142 features of sleep under LD conditions, the presence of two daily peaks in the periodogram (at 12-
143 and 24-h under LD) with approximately 75% of time spent sleeping within a 24-h cycle, to develop
144 our two-process model of fly sleep.
145
146 **Deriving the *Drosophila* two-process model**
147 Although the original two-process model described above (Fig. 1A) produces a single daily peak
148 of sleep, some animals, including humans, often display biphasic/bi-episodic sleep with a nap
149 during mid-day and deeper sleep during the night, much like sleep in *Drosophila* [15,45]. S- and
150 C-process parameters that could produce bimodal sleep (e.g., daytime, and nighttime sleep
151 episodes) were identified in an earlier two-process model [5]. We therefore began building our
152 model with previously published parameter values defining the C-process that were shown to

153 produce bimodal sleep and created various models consisting of different combinations of build-
154 up and decay time-constants of sleep pressure (see Suppl. Fig. 1). It is imperative to explicitly
155 state here that throughout this study we operate under the assumption that the sleep pressure build-
156 up and decay rates themselves are constant over time, which may not be the case in the real world.
157 S-process parameters were determined in humans using EEG-based measures of sleep states [5].
158 In the absence of recognized physiological correlates of fly sleep, the use of behavioral inactivity
159 was the only method by which we could estimate homeostatic parameters in this system. In
160 principle, electrophysiological correlates are a proxy for sleep depth [31], and so are behavioral
161 correlates. Therefore, we use behavioral inactivity states and estimate S-process parameters. For
162 each of these models we first asked if they produced mono-episodic, bi-episodic, pluri-episodic,
163 or arrhythmic/unstructured sleep patterns (see Suppl. Fig. 1). We found that a large region of the
164 parameter space of S-process (all values that S can have, as defined by the input to the model)
165 produced pluri-episodic sleep rhythms (Fig. 2A), meaning they had three or more peaks above the
166 significance line in a periodogram analysis and had three or more episodes of sleep per cycle. A
167 significant region of the parameter space failed to produce coherent sleep rhythms (Fig. 2A),
168 meaning that there were no detectable periodicities revealed by our χ^2 analysis. Smaller regions
169 of the parameter space produced coherent mono-episodic (exactly one sleep episode/24-h) or bi-
170 episodic (exactly two sleep episodes/24-h) sleep rhythms (Fig. 2A).
171
172 Given that we were interested in parameter values that produce two daily episodes of sleep, we
173 subsequently focused on combinations of time constants that yielded exactly two episodes of
174 sleep/24-h cycle. Among these, we quantified the percentage of time spent sleeping per cycle. For
175 each set of build-up and decay parameters, we then compared the values they produced with the

176 percent of time that three fly genotypes, *Canton-S*, w^{1118} and *yw*, slept per cycle (median over all
177 flies/genotype), using sum of squared differences (SSD; see Materials and Methods; Fig. 2B). We
178 found that the lowest SSD (best fit) was attained when the value for a build-up time constant of
179 8.76-h and a decay time constant of 9.51-h (Fig. 2B). Therefore, we chose these parameter values
180 as the best descriptors for daily fly sleep under standard LD cycles. The model generated using
181 these parameter values is shown in Fig. 2C. Though it appears to underestimate daytime sleep and
182 somewhat overestimate nighttime sleep, the percentage time spent sleeping/24-h cycle predicted
183 by the model was ~74.36%, which is close to the percentage of time that the three fly strains spend
184 asleep individually and identical to the average value across the three strains (Fig. 2D). It is curious
185 that the build-up time constant in flies is faster than the decay time constant. This appears to
186 contrast with rodent systems and humans wherein the decay time constant is much faster than the
187 build-up [46]. We think that this could reflect the relative amounts of sleep and wake within a 24-
188 h cycle. Rodents and humans are awake longer than they are asleep, which is the opposite for
189 flies. The short burst of locomotor activity in flies may impose constraints on the rates of sleep
190 pressure changes.
191
192 **Predictions from the two-process model**
193 We built a two-process model of *Drosophila* sleep to systematically predict the effects of altering
194 either the S- or the C-process on fly sleep rhythms. We first asked what would happen to daily
195 sleep if the circadian modulation of sleep thresholds were abolished. To model this, we set the
196 amplitude of the upper and lower thresholds to zero, such that they were held constant at their
197 mean values. Our model made the straightforward prediction that eliminating the contribution of
198 the circadian system would result in ultradian sleep rhythms (Figs. 3A and B). Ultradian rhythms

199 in the locomotor activity of flies with no functional circadian clocks have been reported previously
200 [47,48]. Our model suggests that such rhythms are a predictable consequence of a functional S-
201 process in the absence of circadian modulation of sleep thresholds and predicts ultradian
202 periodicities of sleep of ~10-h in the absence of a functional circadian clock.
203
204 We first visualized this prediction by examining sleep rhythms in wildtype and various loss-of-
205 function clock mutants (*per*^{01}*, tim*^{01}*, clk*^{JRK} *and cyc*^{01}) under constant darkness using continuous
206 wavelet transforms (CWT; a method to detect wide range of periodicities at local timescales) as
207 have been used previously for circadian time-series data (see Materials and Methods) [49–52]. We
208 then used maximum overlap discrete wavelet transforms (mo-DWT) to examine the extent of
209 variance explained by specific ranges of period values for each of these strains as has been done
210 before [53].
211
212 A close inspection of the scalograms in Fig. 3C show the clear presence of strong circadian
213 rhythms (the red band around 24-h) of sleep, in wildtype *CS* flies. Interestingly, clear ultradian
214 sleep rhythms are also visible in these flies. On the other hand, representative scalograms for four
215 loss-of-function clock mutants show no presence of circadian rhythms in sleep, as expected. These
216 flies show significantly stronger ultradian rhythms in sleep (Fig. 3D) as compared to their wildtype
217 counterparts. We then used the mo-DWT to quantitatively characterize the scale-based percentage
218 energy associated with each level of wavelet detail. A wavelet detail is associated with a specific
219 range of periodicities that is defined by $2^j\Delta t$ to $2^{j+1}\Delta t$, where j is the wavelet detail level and Δt is
220 the sampling interval or data collection bin size. Therefore, for data collected in 1-min bins,
221 wavelet detail level 5 would correspond to periodicities ranging from $2^5 \times 1$ = 32-min to $2^6 \times 1$ = 64-

222 min. When we performed such characterization, we found that there was consolidation of energy
223 in wavelet details 3-6 and 10 in the wildtype flies. Given that our data was sampled every minute,
224 wavelet details 3-6 are associated with periods ranging from ~8-min to ~2-h. Wavelet detail 10,
225 as described above, is the circadian band with periods ranging from 17- to 34-h ($2^{10} \times 1$ = 1024-min
226 = 17.067-h to $2^{11} \times 1$ = 2048-min = 34.13-h). We found that wildtype flies had significantly higher
227 percentage of energy associated with wavelet detail 10 – the scale index associated with circadian
228 periodicities – compared to all four loss-of-function clock mutants (Fig. 3E). Importantly, in all
229 four clock mutants, there was significantly higher energy in wavelet details 5 and 6 (corresponding
230 to ~0.5- to ~2-h periods) compared to wildtype flies (Fig. 3E). It is also interesting that there was
231 a broad distribution of ultradian periodicities ranging predominantly from ~16-min to ~2-h (Figs.
232 3C-E) in these flies that were apparent in raw sleep time-series (example shown for per^{01} flies in
233 Suppl. Fig. 2). The range of ultradian periodicities that we detected for sleep was similar to those
234 detected previously for locomotor activity [47,48]. Our results indicate that sleep/wakefulness
235 rhythms are indeed ultradian in loss-of-function clock mutants and are likely driven by a functional
236 S-process in the absence of circadian clock-controlled thresholds, much like a relaxation oscillator.
237 We think that this provides a more parsimonious explanation for the presence of ultradian rhythms
238 in activity than the uncoupling of endogenous ultradian oscillators in loss of function clock mutants
239 [47,48,54].
240

241 **How independent are the S- and C-processes in *Drosophila*?**

242 Based on the persistence of the C-process in the absence of sleep and the maintenance of the S-
243 process in the absence of circadian timekeeping, the two-process model assumes that they are
244 produced by distinct mechanisms. However, it is not clear whether these separate processes

245 operate independently, i.e., without influencing one another's kinetics (reviewed in [11]).
246 Rhythms in the propensity to sleep appear to be independent of the duration of prior waking or
247 sleep duration, implying the independent action of the clock and the homeostat [31]. Furthermore,
248 homeostatic increases in NREM sleep and slow wave activity are observed after sleep deprivation
249 in the absence of the brain's central circadian pacemaker, the suprachiasmatic nuclei (SCN) [55–
250 58]. Though these results support the separateness of the S- and C-processes, recent studies have
251 suggested that these two processes influence one another (reviewed in [11]). For example, loss-
252 of-function modifications to the circadian clock appear to have significant impact on sleep
253 homeostatic markers in mice and flies [32,59–63]. Furthermore, variation in human chronotypes
254 is associated with variation in sleep homeostatic markers (reviewed in [64]). How might the
255 separate S and C processes influence one another in *Drosophila*?
256
257 Thanks to the genetic tools available for the manipulation of the C-process in *Drosophila*, we were
258 able to generate flies with a wide range of circadian periodicities and assess the relationships
259 between the period of the C-process and the amount and waveform of sleep. Thus, we can compare
260 the model's predictions to the experimental effects of C-process manipulation on sleep rhythms
261 (Fig. 4A). First, we recorded locomotor activity in flies with a wide range of circadian periods
262 under DD and constant temperature conditions. We employed five *period* alleles (located on the
263 X-chromosome): per^{T} (free-running period – 15-h; [65]), per^{S} (free-running period – 21-h; [66]),
264 per^{+} (free-running period – 23.5-h), per^{L} (free-running period – 27.75-h; [66]) and per^{01}
265 (arrhythmic; [66]). As expected, these alleles produce significantly different free-running periods
266 (see Table 2). By creating all possible combinations of these alleles (by including heterozygous
267 females), we generated large numbers of flies with a continuous and wide range of free-running

268 circadian periods between ~15- to ~30-h, as previously described by others (see Table 2; [65,66]).
269 We performed this experiment twice, pooled flies from both experiments, and quantified power
270 and hours of sleep/circadian cycle for all rhythmic flies observed (Fig. 4B-C; Tables 2 and 3).
271
272 We also simulated sleep rhythms by altering the free-running periods of the upper and lower
273 thresholds in our model (see Materials and Methods), leaving all other parameters unchanged (Fig.
274 4A; Suppl. Fig. 3); we used these simulations to quantify the power of sleep rhythms and the
275 amount of sleep/circadian cycle. Our model predicted that specific ranges of free-running
276 periodicities would be associated with relatively weak sleep rhythms (Fig. 4D). Specifically, that
277 sleep rhythms would display relatively low periodogram powers for circadian periods between 18-
278 and 22-h, and beyond ~29-h. The model also predicted relatively higher power for periods
279 between 15- to 18-h and 22- to 29-h (Fig. 4D). Though the power of sleep rhythms in our
280 experimental flies did vary markedly across circadian periods, our model's predictions did not
281 match experimental results, which revealed that sleep rhythm power displays considerable
282 variation across the entire range of periodicities examined, with several troughs displayed across
283 the ranges of periods observed (Fig. 4D). When we examined the amount of sleep/circadian cycle
284 in our simulations, we found a monotonic decline in the hours of sleep with lengthening circadian
285 period (Fig. 4E). Once again, our experimental results differed from our model's predictions, with
286 experimental flies displaying lower amounts of sleep than predicted between ~18- and 20-h (Fig.
287 4E).
288
289 We also quantified the relationship between free-running period and the power of locomotor
290 activity rhythms. Interestingly, we found that there is a reasonable match in normalized power of

291 locomotor activity and sleep rhythms in the short period range (between ~15- to ~21-h), but there
292 is quite a mismatch for period values beyond ~21-h (Suppl. Fig. 4A). Consequently, the degree of
293 match between power of locomotor activity time-series and predictions from the model is different
294 from that with sleep time-series (compare Figs. 4D and Suppl. Fig. 4B), thereby highlighting the
295 importance of using sleep time-series to study the circadian regulation of sleep rather than
296 extrapolate from periodogram analyses on locomotor activity time-series. Furthermore, this
297 quantitative relationship between free-running period and power of sleep rhythms was not a
298 consequence of the limitations of the Chi-square periodogram. Analysis using the Lomb-Scargle
299 periodogram revealed a similar relationship between period and power (Suppl. Fig. 5).
300
301 Although the S- and C-processes were initially thought to act without influencing each other's
302 kinetics [31], recent work indicates that they do in fact influence each other [11,32,59–64]. Our
303 model, which assumes that these two processes function independently, failed to precisely predict
304 the relationship between clock speed and sleep rhythm power and amounts of sleep. We therefore
305 sought to adjust the S-process parameters for each free-running period to maximize the fit with
306 our experimental data, once again using the SSD-based approach (Fig. 5A; also see Suppl. Fig. 6).
307 We did this by exploring the build-up and decay rate parameter space for each fly and identified
308 the best fitting set, thereby producing a much better agreement for power and amount sleep
309 between the model and experimental results (see Materials and Methods; Figs. 5B and 5C). The
310 S-process values that produce this fit are shown in Fig. 5D. We found that, there was no linear
311 relationship between free-running period and the build-up time constant of sleep pressure (Fig.
312 5D-left). On the other hand, we found a statistically significant linear relationship between free-
313 running period and sleep pressure decay time constant, wherein flies with longer free-running

314 periods (flies with slower clocks) also have higher time-constants of sleep pressure release (slower
315 decay of sleep pressure; Fig. 5D-right). Therefore, our results show that the rates of the S- and C-
316 processes are indeed interdependent in a way that has implications for our understanding of the
317 regulation of *Drosophila* sleep.
318
319 **To what extent is *Drosophila* sleep a unitary state?**
320 Although sleep has largely been treated as a unitary state in the fly, several independent approaches
321 support the notion that long durations of inactivity correspond to a relatively "deep-sleep" stage
322 [33–39]. For example, metabolic rates of flies that have been inactive for ~35-min are significantly
323 lower than flies that have been inactive for the standard five-minute definition of fly sleep [33].
324 Furthermore, experiments tracking arousal thresholds and brain physiology are consistent with
325 deeper sleep intensities when flies have been inactive for ~30-min [34].
326
327 The original two-process model made predictions regarding the amount of total sleep time by
328 modeling the S-process based on the exponential decay of the power of sleep EEG (0.75- to 25-
329 Hz). This wide range of EEG frequencies corresponds to all sleep types, i.e., slow wave and REM
330 sleep. Interestingly, the decay constant derived from such a wide range of EEG frequencies was
331 very similar to the constant derived from slow wave sleep alone (0.5- to 2-Hz) [5,67], thereby
332 suggesting that although the two-process model accounts for total sleep, the S-process properties
333 are most closely reflected by NREM sleep. Since decay rate constants best reflect NREM sleep,
334 we assessed the degree to which our model predictions would describe empirical data when
335 increasing durations of inactivity were used as the defining criterion for a sleep like state, thereby
336 biasing our sleep analysis to longer, presumably deeper, bouts of sleep in experimental flies.

337 Because recent studies in flies (discussed above) have established a clear correlation between the
338 duration of inactivity and the depth of sleep, we use the term "deep" to refer to sleep bouts that are
339 longer than the traditional unitary five-minute inactivity definition of fly sleep. Similar
340 associations between sleep consolidation (number of spontaneous brief awakenings) and sleep
341 pressure (measured using slow wave activity) have also been reported in rodent models [68],
342 therefore suggesting that this association is likely a conserved phenomenon.
343
344 We systematically altered the inactivity duration definition of sleep, i.e., the duration of inactivity
345 used to define the sleep state and examined the correlation between the amount of time flies spent
346 sleeping and our model's prediction (Figs. 6A-B). Traditionally, any bout of inactivity that is five
347 minutes or more is defined, in flies, as sleep. The correlation between our model's prediction and
348 measurements of amount of time spent sleeping in our series of allelic combinations of *period*
349 changes very little with increasing inactivity definitions, at least until the criterion for sleep reaches
350 30-min of inactivity (Figs. 6A-B). This result implies that shorter bouts of inactivity contribute
351 very little to how the amount of time spent sleeping varies with circadian period.
352
353 To further test this idea, we performed the same analysis as above but with specific ranges of
354 inactivity durations used for the definition of sleep (see Materials and Methods for details). For
355 instance, a five to 30-minute interval definition of sleep would mean that any bout of inactivity
356 that is equal to or more than five minutes but fewer than 30 minutes would be considered sleep.
357 We found that the correlation between empirical results and model predictions is relatively low
358 when five to 10, 20 or 30 minutes of inactivity were used as the definitions of sleep (Fig. 6B).
359 Correlations improved a little when the inactivity definition was set to 30 to 60 minutes and became

360 fairly high when set to 30 to 120 minutes (Fig. 6B). These results suggest that our model can
361 account for a large part of the relationship between circadian period and amounts of deep sleep
362 and are consistent with recent work suggesting that different durations of inactivity are unlikely to
363 represent the same state with respect to sleep in *Drosophila* [33–39].
364

365 **An independent test confirms that faster running clocks also have altered sleep homeostatic**
366 **properties.**

367 In fitting our two-process model to sleep observed over a range of circadian periods, our results
368 indicate that, as previously suggested, the S- and C-processes influence one another. We found
369 that changes in the decay time constant of the S-process accompanied changes in the free-running
370 period of the C-process (Fig. 5D-right). We therefore sought to independently test this idea that
371 flies with shorter free-running periods will also have faster decay of sleep pressure (see Fig. 5D-
372 right). To look at this relationship more closely we examined deep sleep (30-minutes or longer of
373 inactivity) in per^{+} and per^{S} flies under conditions in which the C-process had been rendered
374 arrhythmic, a condition which reveals ultradian rhythms driven by the operation of process S alone
375 (see Figs. 3 and 7A). Our results described above (see Fig. 5D) leads to the following predictions
376 in the absence of circadian cycling of sleep thresholds (therefore, no circadian gating of sleep): (i)
377 ultradian rhythms in sleep/wake will be faster in per^{s} mutants compared to per^{+} flies, (ii) total
378 amount of sleep would be lower in per^{s} mutants compared to per^{+} flies, and (iii) number of sleep
379 bouts will be higher in per^{S} mutants compared to per^{+} flies per unit time (Fig. 7A). Based on the
380 results in the previous section (Fig. 6), we argue that examining deep sleep in these flies will
381 perhaps be a closer reflection of process S.
382

383 *Drosophila* is arrhythmic under continuous white light (LL) owing to the constitutive
384 CRYPTOCHROME mediated degradation of TIMELESS [69–71]. Thus, LL conditions provide
385 a convenient means of abolishing the cycling of sleep thresholds (C-process). We therefore
386 examined sleep behavior in per^S and per^+ (*CS*) flies under LL and examined longer bouts
387 (presumably deeper, homeostatic) of sleep (see results above and Fig. 7A). As expected, over the
388 duration of 15 days under constant white light, there was a clear absence of any circadian
389 rhythmicity in both per^+ and per^S flies (Fig. 7B). Employing recently described methods [53,72],
390 we identified three specific bands of ultradian periodicities using mo-DWT (see Materials and
391 Methods) that account for the majority of spectral variance in the sleep timeseries of per^+ and per^S
392 flies (Figs. 7C and 7D). These three ranges of periods were 1.07-2.1-h (τ_s *or* τ_{short}), 2.1-4.27-h (τ_m
393 *or* τ_{medium}) and 4.27-8.53-h (τ_l *or* τ_{long}; Figs. 7C and 7D). We analyzed the period values in these
394 categories separately for both these strains. We found that, as predicted, per^S had significantly
395 faster ultradian periods in the τ_s category (Fig. 7E). There was no significant between-strain
396 difference in periods in the other two period categories (Fig. 7E). Furthermore, we found
397 statistically significantly reduced total sleep (Fig. 7F) and increased bout numbers (Fig. 7G) in
398 per^S flies compared to per^+ flies. Our results, therefore, support *all three* predictions from the
399 model, thereby lending support to the notion that shorter free-running periods are indeed associated
400 with faster rates of sleep pressure decay.
401

402 **Discussion**

403 Through this manuscript, we show that an examination of the circadian regulation of sleep must
404 involve the use of time-series analyses on sleep data rather than relying on locomotor activity data
405 (Fig. 1). We have created tools to make such analyses accessible to a wider community of sleep
406 researchers through an open-access R package [40] (different from our recently published
407 MATLAB software, PHASE [73]; https://cran.r-project.org/web/packages/phase/index.html). By
408 utilizing these tools, we derive a two-process model of sleep regulation for flies that is capable of
409 accounting for the bi-episodic nature of fly sleep and the percentage of time spent sleeping under
410 LD12:12 (Fig. 2). In addition, we show that ultradian rhythms in sleep are detectable in flies
411 whose circadian sleep thresholds do not oscillate (Fig. 3). We then show that a two-process model
412 in which the circadian clock speed and rates of the S-process do not covary is incapable of
413 explaining *Drosophila* sleep rhythm strength and amounts across a wide range of periodicities
414 under constant darkness (Fig. 4). However, covarying sleep homeostatic parameters along with
415 the free-running period produces much better fits with experimental observations (Fig. 5) and
416 suggests that circadian clock speeds are strongly correlated with the sleep pressure decay rate (Fig.
417 5). Furthermore, we show that our model predictions regarding the relationship between circadian
418 period and amounts of sleep are in agreement with longer, deeper sleep bouts in flies, suggesting
419 that short bouts are dispensable for capturing this relationship (Fig. 6). Using such longer bouts
420 of sleep, we show that indeed per^S flies exhibit several major properties of a homeostatic system
421 that is characterized by faster decay of sleep pressure compared to wildtype flies (Fig. 7). These
422 results underscore the utility of a formal two-process model for understanding the regulation of
423 sleep in *Drosophila*.

424

425 *On ultradian rhythms in sleep and the inter-relationship between circadian period and rates of*
426 *homeostatic processes*
427 The theoretical framework around Borbély and Daan's two-process models has played a critical
428 role in the advances made in our understanding of mammalian sleep [2,4–7]. The conservation of
429 sleep-like states across taxa and the power of *Drosophila* as a genetically tractable organism has
430 made the fly a fruitful model system for the study of sleep regulation. However, the field of fly
431 sleep has not benefitted from the strong theoretical framework provided by a formal two-process
432 model. The appropriateness of this model as a framework for the investigation of fly sleep is
433 exemplified by its prediction that ultradian sleep rhythms are a consequence of a functional S
434 process in absence of oscillating thresholds (Figs. 3A and 3B). The two-process model of
435 mammalian sleep has been adjusted to account for the presence of cycling NREM and REM sleep
436 states in mammals, which produce ultradian EEG rhythms during bouts of sleep [74–76].
437 However, the ultradian changes in sleep state produced by normal sleep cycles occur during the
438 circadian clock timed daily window of sleep and are therefore distinct from the ultradian rhythms
439 in sleep bouts predicted by two-process models when the circadian cycling of sleep thresholds is
440 abolished. Mistlberger and co-workers (1983) [77] detected the presence of ultradian rhythms in
441 wheel running activity when the suprachiasmatic nuclei were bilaterally ablated, thereby
442 abolishing circadian timekeeping. However, these ultradian rhythms were not explained in the
443 context of the two-process model.
444
445 Previous work on loss-of-function *period* mutants detected the presence of ultradian rhythms in
446 locomotor activity [47,48], which were hypothesized to be due to an uncoupling of ultradian
447 oscillators [47,54,78]. However, our results, which demonstrate the presence of such rhythms in

448 a range of loss-of-function clock mutants (Figs. 3D and 3E), suggest that they are a simple
449 consequence of the rise and fall of sleep pressure between non-oscillating sleep thresholds, akin to
450 an hourglass system as has been previously suggested [79] or a relaxation oscillator. It is important
451 to note here that although the model predicts an ultradian sleep rhythm of ~10-h, our results in
452 clock mutant flies reveal much ultradian shorter periods, albeit with a wide distribution of periods
453 that lack the stability of a robust circadian oscillator. Among the possible explanations for this
454 discrepancy are a reduced distance between the thresholds in the mutants, a steeper rise or decay
455 of sleep pressure, or non-oscillating but unstable thresholds in loss of function clock mutants. The
456 large variance in ultradian periodicities that are detected may also be a consequence of independent
457 stochastic fluctuations of the upper and lower thresholds and the distance between them. Indeed,
458 a combination of all such factors may be at play. Moreover, enhanced sensitivity of per^{01} mutants
459 to sleep deprivation has been reported previously, suggesting a pleiotropic effect of the loss of
460 *period* on the sleep homeostat [32]. Similar pleiotropic effects may also govern the S-process of
461 other loss-of-function clock mutants, contributing to this large variation in detected ultradian
462 periodicities. However, the quantifiable presence of such ultradian oscillations in sleep (Fig. 3)
463 and the possibility of detailed characterization of their properties (Fig. 7) under conditions of non-
464 cycling upper and lower thresholds promises to be a useful new approach for the study of the
465 mechanisms regulating process S that are highly likely to complement work employing sleep
466 deprivation to examine the homeostatic regulation of sleep.
467
468 The detectable effects of faster decay of sleep pressure in per^{S} flies under LL conditions (Fig. 7)
469 is remarkable because PER protein is constitutively low under continuous light [80]. This implies
470 that there may be a fundamental relationship between clock speed and the rates of change of the

471 sleep homeostatic system. It is possible that the free-running circadian period present during
472 development shapes homeostatic systems to coordinate the build-up and/or decay of sleep pressure
473 with clock speed. It is also possible that *period* alleles have different effects on the homeostatic
474 control of sleep via epigenetic mechanisms. Recent studies have reported differential epigenetic
475 regulation associated with cell populations with divergent periods and distinct levels of clock gene
476 expression [81,82]. Our results in flies may be broadly relevant to animal sleep regulation, as
477 similar results have been reported in humans [64]. Specifically, the human $PER3^{5/5}$ polymorphism
478 is highly enriched in morning chronotypes, and such early types also have faster-running circadian
479 clocks. Remarkably, $PER3^{5/5}$ individuals experience higher sleep pressures and a faster build-up
480 of non-REM activity during sleep deprivation compared to another human *PER* polymorphism,
481 $PER3^{4/4}$ [64,83].
482
483 Previous studies that simulated S-process parameters in rodent models found considerable
484 variation in the time constants of build-up and decay rates of the homeostatic sleep drive across
485 species and among strains of the same species [5,46,84]. We compared these values and the time
486 constants derived from human EEG data and found that rodent models have faster build-up and
487 decay rates of the S-process compared to humans. We then looked at free-running periods of a
488 commonly used mouse strain and that of humans and found that mice have faster running circadian
489 clocks than humans [85,86]. This is consistent with our conclusion that speed of the circadian
490 clock likely affects the rates of S-process increases and decreases. The faster build-up of sleep
491 pressure than its decay in flies may be a necessary constraint (given the choice of circadian clock
492 parameters chosen in this study) for facilitating two bouts of sleep/cycle in flies, where one bout
493 is considerably longer than the other.

494

495 *The utility of the two-process model of fly sleep for understanding previous findings and the*
496 *generation of new testable hypotheses*

497 The integration of this quantitative model with previous work examining the effects of specific
498 clock neuron types on sleep and the daily timing of neural activity they display, offers a unique
499 and powerful framework for understanding the neural basis of circadian sleep regulation in the fly.
500 An examination of our model in the context of the growing body of knowledge regarding the
501 relationships between circadian clock neurons and sleep timing leads to specific and empirically
502 testable hypotheses that have not emerged from current models. Furthermore, the roles of
503 circadian clock neurons in sleep control have not been investigated in the context of cycling sleep
504 thresholds.

505

506 Under normal circumstances (i.e., the absence of physiological or social challenges), our model
507 suggests that the onset of daytime sleep is timed by the event of the S-process hitting the rising
508 phase of the upper threshold (Fig. 8A). The onset of nighttime sleep, on the other hand, is timed
509 by the falling phase of the upper threshold (Fig. 8A). Both, the morning, and evening bouts of
510 wakefulness appears to be timed by the rising phases of the lower threshold (Fig. 8A). The falling
511 phase of the lower threshold appears to support the consolidation and maintenance of nighttime
512 sleep (Fig. 8A). Work over the last decade has assigned sleep- or wake-promoting functions to
513 specific classes of circadian clock neurons (reviewed in [14]). For example, the small ventral
514 lateral neurons (s-LNvs) and the dorsal lateral neurons (LNds) are thought to be wake-promoting,
515 whereas the dorsal neuron classes are thought to be sleep-promoting (reviewed in [14,16]). In

516 these cases, the daily timing of neural activity displayed by these cell types, as measured by relative
517 Ca^{2+} levels, fits these proposed roles in sleep control well (Fig. 8A).
518
519 The s-LNvs display Ca^{2+} peaks that coincide with the morning bout of locomotor activity, the
520 LNds display peaks that coincide with the evening bout of locomotor activity, and the DN-1 and
521 DN-3s display their highest Ca^{2+} levels during the nighttime bout of sleep [87]. Integrating these
522 patterns with our two-process model suggests that the s-LNvs control the timing of morning
523 wakefulness by driving the initial rise of the lower sleep threshold, that the LNds promote the
524 timing of evening wakefulness by the continued rise in the in the lower sleep threshold, and that
525 the DNs promote the maintenance of nighttime sleep by driving the fall of the lower threshold
526 throughout the night (Fig. 8A). Though this model explains daily sleep and wake patterns well,
527 the timing and duration of daytime and nighttime sleep windows may also be controlled in other
528 ways. For example, the distance between the two thresholds, the phase relationships between the
529 two thresholds, or the relative amplitudes of the upper and lower threshold cycles might all be
530 modulated by the circadian system to shape the timing and amount of sleep. These possibilities
531 should be explored in future studies.
532
533 To test the utility of overlaying circadian clock neuron calcium activity and the two-process model
534 for explaining previously published results and for generating new testable predictions, we
535 considered the effects of DN neurons manipulation from previous studies. These studies have
536 reached opposing conclusions regarding the role of the dorsal neurons 1 (DN-1) in sleep
537 regulation: they have been proposed to be both wake- [88,89] and sleep-promoting [90,91].
538 Though these apparently incompatible conclusions may ultimately be explained by the different

539 technical approaches used in these studies, the two-process model provides an explanation for how
540 similar experimental manipulations of the same clock neuron classes might lead to contradictory
541 conclusions. According to Liang et al., 2016 [87] the DN1ps display peak levels of neuronal
542 activity in the middle of the night, a time associated with nighttime sleep, and a pattern that would
543 appear to fit a sleep promoting role for these clock neurons. However, our model predicts that the
544 effect of acutely exciting the DN-1ps would depend on the timing of the manipulation on neural
545 signaling. For instance, if the DN-1ps promote the fall in the lower sleep thresholds, as suggested
546 by our hypothesized relationship between the sleep thresholds and DN-1p Ca^{2+} profiles (Fig. 8A),
547 exciting these neurons during the late afternoon would lead to an early and prolonged fall in the
548 lower threshold (Fig. 8B). According to the model, this would increase daytime sleep by a delayed
549 offset of daytime sleep and decrease nighttime sleep by causing a delayed onset and early offset
550 of nighttime sleep (Fig. 8B). An increase in daytime sleep was used by Guo et al., 2016 [91] to
551 support the conclusion that exciting DN-1ps promotes sleep. In contrast, Kunst et al., 2014 [89],
552 present evidence for increased daytime sleep (Fig. 8B), but also describe a reduction in nighttime
553 sleep, which, while not observed by Guo et al., 2016 [91], is predicted by our synthesis. Next, we
554 asked what would happen to endogenous sleep rhythms if the DNs are inhibited. We model this
555 by not allowing the lower threshold to fall below baseline (Fig. 8C). Our model predicts that
556 inhibition of DNs would lead to disrupted sleep rhythms under constant conditions (Fig. 8C).
557 Future work, employing time-series analysis of long, deep sleep bouts, will allow us to test
558 numerous predictions provided by a synthesis of the two-process model and the daily patterns of
559 clock neuron activity. This will provide a new approach to the examination of the circadian
560 regulation of sleep in the brain.
561

562 *Speculations and Concluding Remarks*

563 Our time-series analysis of *Drosophila* sleep detected the presence of ultradian periodicities under
564 constant conditions in both wildtype flies and mutants lacking circadian timekeeping. Might these
565 ultradian sleep rhythms reflect a cycling through different stages of sleep during the two daily
566 bouts of sleep? Might such cycling occur at specific times of the circadian cycle? Answers to
567 these questions await further detailed analyses of sleep time-series using the methods of analysis
568 described here, all of which are freely available.

569

570 We have synthesized a formal, quantitative model of sleep regulation in *Drosophila* and have used
571 it to guide the development of empirically testable hypotheses regarding the circadian control of
572 sleep. We've also made this accessible to the wider sleep community by generating a Shiny-based
573 GUI to facilitate simulations. We propose that this model can serve as a powerful framework for
574 investigating the contributions of the various clock neuron to sleep regulation. The predictions
575 made by this model were supported by experimental results, which were reminiscent of human
576 studies on the relationships between circadian timekeeping and the homeostatic control of sleep.
577 This suggests that the relationships between these two processes discovered in the fly will prove
578 to be broadly relevant to our understanding of sleep regulation in animals. Our analysis also
579 suggests that simple changes to the way we define sleep-like states will support new insights into
580 the homeostatic regulation of fly sleep. Because the two-process model has been a major driving
581 force for our understanding of sleep regulation in humans, we propose that adopting the two-
582 process model to other genetically tractable experimental systems will support significant new
583 insights into the molecular and neural mechanisms controlling sleep.

584

585 ## Materials and Methods

586 **Fly husbandry**

587 *Canton-S (CS*; BDSC stock number: 64349*)*, *white*^{1118} (*w*^{1118}; [92]), *yellow, white* (*yw*; BDSC stock
588 number: 1495), *period*^{TAU} (*per*^{T}; [65]), *period*^{SHORT} (*per*^{S}; [66]), *period*^{LONG} (*per*^{L}; [66]), and
589 *period*^{01} (*per*^{01}; BDSC stock number: 80928), *timeless*^{01} (*tim*^{01}; BDSC stock number: 80930),
590 *clock*^{JRK} (*clk*^{JRK}; BDSC stock number: 80927) and *cycle*^{01} (*cyc*^{01}; BDSC stock number: 80929)
591 flies were used for the behavioral experiments reported in this manuscript. *CS* flies are also
592 referred to as *period*$^{+}$ (*per*$^{+}$) or wildtype interchangeably throughout the text, as all the *period*
593 alleles used here were in a *CS* background. Flies were reared on Corn Syrup/Soy media made by
594 Archon Scientific (Durham, North Carolina). Flies were approximately five days old on day one
595 of all behavioral experiments.

596

597 **Generation of flies with a wide range of free-running periods**

598 To generate flies with a wide range of period values, virgin females and males from all five *period*
599 allele cultures (*per*^{T}, *per*^{S}, *per*$^{+}$, *per*^{L} and *per*^{01}) were collected over the span of approximately five
600 days. Reciprocal crosses were performed, resulting in a total of 25 distinct crosses. Male and
601 female offspring from each of these 25 crosses, representing 50 distinct sex and genotype
602 combinations (see Tables 1 and 2), were collected and assayed for locomotor activity as described
603 below.

604

605 **Assay of locomotor activity**

606 Locomotor activity was recorded using the *Drosophila* Activity Monitor (DAM) system
607 (Trikinetics, Waltham, MA; https://trikinetics.com). Beam crossing counts were collected every

608 minute for all experiments. Flies were recorded under LD12:12 cycles, constant darkness (DD) or
609 constant bright white light (LL). In all experiments reported in this manuscript, flies were assayed
610 under 25 °C and the intensity of white light was between ~400 and ~500 lux.
611
612 **Data analyses and visualization**
613 *Circadian time-series analysis of Drosophila sleep*
614 Locomotor activity of approximately 32 each of *CS*, w^{1118} and *yw* male flies was recorded under
615 LD12:12 for nine days, after which activity was recorded under constant darkness (DD) for seven
616 days. Beam crossing data from these recordings were used to determine the pattern and amount
617 sleep for each fly. Individual fly locomotor activity and sleep time-series data, binned in 1-minute
618 intervals, were subjected to (Chi-square) χ^2 or Lomb-Scargle periodogram analyses.
619
620 *Calculating the percentage/amount of time spent sleeping*
621 For fly sleep under LD cycles, the percentage of time spent sleeping was calculated by first
622 computing the total sleep over the entire duration of the experiment for each fly (last four cycles
623 of entrainment). This total was divided by the number of 24-h cycles (i.e., 4), and then multiplied
624 by $\frac{100}{24}$.
625
626 For flies under DD and for simulations of free-running sleep, the fly wise total amount of sleep (in
627 hours) over the entire duration of the experiment or simulations was calculated. Because flies with
628 different free-running periods would differ in the number of sleep/wake cycles experienced during
629 free run – for example periods shorter than 24-h would complete more than 10 cycles in 10, 24-h

630 days and clocks with periods longer than 24-h would complete fewer – we accounted for clock
631 speed in our calculations. Therefore, all our estimates of sleep are hours of sleep/circadian cycle.
632
633 *Continuous wavelet transforms as a tool to identify ultradian rhythms in sleep*
634 Biological oscillations are often non-stationary time-series, i.e., their amplitude and period vary
635 significantly over time. Such variations are often not of interest when estimating period and power
636 of circadian rhythms. However, when attempting to identifying multiple periodic components
637 from non-stationary time-series, traditional methods like the χ^2 periodogram often fail to
638 accurately reflect the presence of multiple periodicities, especially when they are restricted to
639 certain windows of time throughout the length of the time-series [41,49,51]. Recently, analytical
640 tools to resolve circadian rhythms in both the time and frequency domain (i.e., provides period and
641 amplitude information locally over a long time-series) have been developed and utilized [49–52].
642 We made use of one such tool, the continuous wavelet transforms (CWT), to visually examine
643 periodic components in sleep time-series of our flies. We used functions from the WaveletComp
644 package in R, which use a Morlet mother wavelet and resolves biological time-series in the time-
645 frequency domain [49,93]. Complex-valued wavelet transforms such as the Morlet wavelet are
646 useful because they provide amplitude and phase over time and generally preserve information
647 about these locally [49,93]. To assess the presence of ultradian rhythms, sleep timeseries for all
648 our genotypes for varying definitions of sleep were calculated in bins of 60-minutes. CWT were
649 carried out and significance of detected periodicities were tested against a null hypothesis of "no
650 periodicity" using shuffled timeseries. The null distributions were generated based on 1000
651 simulations of such shuffled timeseries. In order to quantitatively compare features of periodicities
652 between genotypes (as shown in Figs. 3 and 7), we used a modified pipeline based on recent

analytical developments [72]. We first performed discrete wavelet transforms (DWT) on 1-min binned sleep timeseries on our genotypes using a Daubechies wavelet of filter length 12 using the functions from the package "wavelets" on R [94]. We then computed the percentage of spectral variance accounted for by each level of the scale index as has been done previously [53,72]. Based on this, we identified three period bands of relevance in Fig. 3E (~0.5-~1-h, ~1-~2-h and ~17-~34-h) and Figs. 7C and 7D (~1.07-~2.1-h, ~2.1-~4.27-h and ~4.27-~8.53-h). We used 1-min intervals to compute the DWT to get the maximum resolution in identifying period bands corresponding to each wavelet detail (see Results).

In order to compare period values among genotypes within specific period bands (as in Fig. 7E), we revisited the identified periodicities from the CWT. In the interest of computation time, we performed the above-described continuous wavelet transforms on flies of *CS* and per^S flies using 15-min binned sleep timeseries, and the significance of detected periodicities were based on 100 simulations of shuffled timeseries. We then computed median period and power for each fly in each of the three identified period bands after accounting for edge effects [72]. These values were then used to make between genotype comparisons. Statistical significance between genotypes were tested using bootstrapped *t*-tests with 10000 bootstrap replicates and were carried out using functions from the package MKinfer on R [95].

Time-series analysis of various definitions of sleep

Traditionally, *Drosophila* sleep has been defined as any bout of inactivity (usually the absence of beam crossings in DAM monitors) that lasts five minutes or more [12,13,15]. Though this method has been shown to overestimate the amount of sleep [96], its easy implementation and consistency

676 over decades of research have made it an integral approach to measuring sleep in the fly. In
677 addition to the traditional definition of sleep, we systematically changed the inactivity duration
678 criterion for sleep to examine how the temporal regulation of sleep was affected by biasing our
679 analysis to longer bouts of inactivity or specific ranges of inactivity. For example, a ten-minute
680 inactivity duration definition of sleep would mean that any bout of inactivity lasting ten minutes
681 or more would be considered sleep and subjected to time-series analysis, whereas a five to 20-
682 minute definition of sleep would mean only bouts of inactivity that are more than five minutes but
683 fewer than 20 minutes would be considered as sleep and subject to the analysis. These time-series
684 were then subjected to Chi-square or Lomb-Scargle periodogram analyses, as described above.
685
686 *Figure generation*
687 All figures were generated using custom scripts in R. We used the "wesanderson" package [97]
688 to generate color palettes used in the figures, except in case of the acto-/somnograms, time-series
689 plots in Fig. 1, the CWT spectrograms, and the Suppl. Figs. In these three cases, default color
690 palettes were used to generate the plots.
691
692 **Creating the two-process model and generating predictions**
693 A major strength of the original two-process model was that it used EEG data to derive the
694 parameter values of the sleep homeostat [4,5]. Because no equivalent physiological correlate of
695 sleep is, as yet widely employed in flies, we relied on best-fitting approaches to find model
696 parameters that best explain the waveform and amount of sleep in *Drosophila*. The basic structure
697 of the two-process model used here is taken from a two-process model proposed by Daan et al., in
698 1984 [5]. The upper and lower thresholds are modeled as simple sinusoidal oscillations:

$$U = M_u + A_u \cos(\omega_u t + \varphi)$$

$$L = M_l + A_l \cos(\omega_l t + \varphi)$$

U and L are the upper and lower thresholds, respectively. M_u and M_l are the mean levels around which U and L oscillate. A_u and A_l are the amplitudes of the upper and lower threshold oscillations. ω_u and ω_l are the angular velocities of the oscillations. The angular velocities are determined by the period of the oscillation, which is expressed as $\omega = \frac{2\pi}{\tau}$. τ is the period of the oscillation, which in this study, was fixed at the same value for both thresholds. φ is the phase angle by which the starting phase of the oscillations are adjusted and was likewise fixed at the same value for the upper and lower thresholds. The build-up of sleep pressure is modeled as:

$$s_t = 1 - i \times (1 - s_{t-1}); i = e^{-\Delta t / t_i}$$

s_t is the value of sleep pressure at any given time t. i is the parameter determining the increase of build-up of sleep pressure. s_{t-1} is the value of sleep pressure at any given time $t - 1$. Δt is the sampling interval (or bin size) for the simulations. This was set at 1-min because that is the resolution at which behavioral records were collected from our flies. t_i was the build-up time constant. The decay of sleep pressure is modeled as:

$$s_t = \delta s_{t-1}; \delta = e^{-\Delta t / t_\delta}$$

721 s_t is the value of sleep pressure at any given time t. δ is the decay rate of sleep pressure. s_{t-1} is
722 the value of sleep pressure at any given time $t-1$. Δt is the sampling interval for the simulations.
723 t_δ was the decay time constant. The upper and lower thresholds were computed for the entire
724 duration of the simulation. The simulations for sleep pressure build-up and decay were performed
725 under the following conditions: at every time-step t, the program will increase sleep pressure as
726 long as its value at the previous time-step $(t-1)$ was lower than the higher threshold at t. If at
727 $t-1$, the sleep pressure value is higher than the upper threshold at time t, the program will release
728 the sleep pressure at t. Sleep pressure will continue to be released (i.e., fall) until it reaches the
729 lower threshold value at t. The model was allowed to run for a duration of 60 days. The first 30
730 days of the simulation were discarded from analyses to remove potential transient behaviors. The
731 remaining 30 days were used for all analyses. The window of time in the simulation where sleep
732 pressure is being released is designated as the window of sleep. Using this window, the number
733 of hours of sleep predicted by the model was computed for all conditions. This allowed for the
734 estimation of percentage of time spent sleeping or the amount of sleep/circadian cycle. The sleep
735 pressure time-series thus generated was subjected to χ^2 periodogram analyses to produced
736 estimates of number of peaks in the periodogram and to assess the power of sleep rhythms. Power
737 was defined as the height of the periodogram peak above the 0.05 significance cut-off. To facilitate
738 easy access to predictions from these simulations, we have created a GUI which is available here:
739 https://abhilashlakshman.shinyapps.io/twoprocessmodel/
740
741 *Measuring sum of squared differences (SSD)*
742 The S-process parameters that best recapitulated the waveform and amount of fly sleep were
743 estimated using a sum of squared differences approach. For each combination of sleep pressure

744 build-up (t_i) and decay (t_δ) parameters, we asked if the model produced two coherent peaks of
745 sleep, and, if so, we assessed the difference between the % time spent sleeping predicted by the
746 model and that of our experimental flies and this difference was squared to account for negative
747 values. For the results reported in Fig. 2, SSD values were calculated across the three genotypes
748 (using population averages; therefore, there are no estimates of errors on these parameter values)
749 and, in the case of fitting reported in Fig. 5, SSD was computed for both the amount of time spent
750 sleeping and for the normalized power of the sleep time-series periodogram. Given this approach,
751 there is no good way to statistically distinguish neighboring points in the parameter space, except
752 to choose the one with the minimum SSD. Any prediction that is close to empirical value would
753 have small differences with the experimental data and consequently would have low SSD values.
754 Therefore, the build-up and decay rates that together yielded the minimum SSD were considered
755 the best-fitting parameters for our two-process models. See Suppl. Figs. 1, 3 and 6 for a guide to
756 the algorithms for our model outputs. All our simulations were run on a 32-core AMD RYZEN
757 Threadripper processor.
758

759 **Acknowledgements**

760 This work was supported by a grant from the National Institute of Neurological Disorders and
761 Stroke (R01NS077933) and start-up funds provided by the State of New York. We thank Michael
762 Rosbash, Paul Hardin, Amita Sehgal, Patrick Emery, and Ralf Stanewsky for fly lines. We would
763 also like to thank Aliya Fisher and Matthew Ciolkowski for technical support. We are grateful to
764 Bill Joiner, Joydeep De, Meilin Wu, and Paul Franken for useful discussions of the work presented
765 in this study. Finally, we thank Maria de la Paz Fernández, Matthew Ciolkowski, Budha
766 Chowdhury, and Robert Veline for providing useful feedback on the manuscript. We would also

like to extend our thanks to two anonymous reviewers for carefully reading a previous version of this study and providing valuable feedback.

References

[1] Campbell SS, Tobler I. Animal sleep: A review of sleep duration across phylogeny. Neurosci Biobehav Rev 1984;8. https://doi.org/10.1016/0149-7634(84)90054-X.

[2] Alexander Borbély. A two process model of sleep regulation. Hum Neurobiol 1982.

[3] Moore-Ede MC, Czeisler CA. Mathematical models of the circadian sleep-wake cycle. New York: Raven Press; 1984.

[4] Serge Daan, Domien Beersma. Circadian gating of human sleep-wake cycles. In: Moore-Ede MC, Czeisler CA, editors. Mathematical models of the circadian sleep-wake cycle, New York: Raven Press; 1984, p. 129–57.

[5] Daan S, Beersma DGM, Borbely AA. Timing of human sleep: recovery process gated by a circadian pacemaker. Am J Physiol 1984;246. https://doi.org/10.1152/AJPREGU.1984.246.2.R161.

[6] Alexander Borbély. The two-process model of sleep regulation: Beginnings and outlook. J Sleep Res 2022:1–8.

[7] Borbély AA, Daan S, Wirz-Justice A, Deboer T. The two-process model of sleep regulation: a reappraisal. J Sleep Res 2016;25:131–43. https://doi.org/10.1111/JSR.12371.

[8] Booth V, Diniz Behn CG. Physiologically-based modeling of sleep-wake regulatory networks. Math Biosci 2014;250:54–68. https://doi.org/10.1016/J.MBS.2014.01.012.

[9] Dijk DJ, Kronauer RE. Commentary: models of sleep regulation: successes and continuing challenges. J Biol Rhythms 1999;14:571–5. https://doi.org/10.1177/074873099129000902.

[10] Beckwith EJ, French AS. Sleep in Drosophila and Its Context. Front Physiol 2019;10. https://doi.org/10.3389/fphys.2019.01167.

[11] Deboer T. Sleep homeostasis and the circadian clock: Do the circadian pacemaker and the sleep homeostat influence each other's functioning? Neurobiol Sleep Circadian Rhythms 2018;5. https://doi.org/10.1016/j.nbscr.2018.02.003.

[12] Hendricks JC, Finn SM, Panckeri KA, Chavkin J, Williams JA, Sehgal A, et al. Rest in Drosophila Is a Sleep-like State. Neuron 2000;25:129–38. https://doi.org/10.1016/S0896-6273(00)80877-6.

[13] Shaw PJ, Cirelli C, Greenspan RJ, Tononi G. Correlates of Sleep and Waking in Drosophila melanogaster. Science (1979) 2000;287:1834–7. https://doi.org/10.1126/SCIENCE.287.5459.1834.

[14] Shafer OT, Keene AC. The Regulation of Drosophila Sleep. Current Biology 2021;31:R38–49. https://doi.org/10.1016/J.CUB.2020.10.082.

[15] Shafer OT, Keene AC. The Regulation of Drosophila Sleep. Curr Biol 2021;31:R38–49. https://doi.org/10.1016/J.CUB.2020.10.082.

[16] Artiushin G, Sehgal A. The Drosophila circuitry of sleep–wake regulation. Curr Opin Neurobiol 2017;44. https://doi.org/10.1016/j.conb.2017.03.004.

[17] Helfrich-Förster C. Sleep in Insects. Annu Rev Entomol 2018;63. https://doi.org/10.1146/annurev-ento-020117-043201.

[18] Donlea JM, Thimgan MS, Suzuki Y, Gottschalk L, Shaw PJ. Inducing sleep by remote control facilitates memory consolidation in Drosophila. Science (1979) 2011;332. https://doi.org/10.1126/science.1202249.

[19] Liu S, Liu Q, Tabuchi M, Wu MN. Sleep drive is encoded by neural plastic changes in a dedicated circuit. Cell 2016;165. https://doi.org/10.1016/j.cell.2016.04.013.

[20] Donlea JM, Pimentel D, Talbot CB, Kempf A, Omoto JJ, Hartenstein V, et al. Recurrent Circuitry for Balancing Sleep Need and Sleep. Neuron 2018;97. https://doi.org/10.1016/j.neuron.2017.12.016.

[21] Pimentel D, Donlea JM, Talbot CB, Song SM, Thurston AJF, Miesenböck G. Operation of a homeostatic sleep switch. Nature 2016;536. https://doi.org/10.1038/nature19055.

[22] Liu Q, Liu S, Kodama L, Driscoll MR, Wu MN. Two dopaminergic neurons signal to the dorsal fan-shaped body to promote wakefulness in Drosophila. Current Biology 2012;22. https://doi.org/10.1016/j.cub.2012.09.008.

[23] Donlea JM, Pimentel D, Miesenböck G. Neuronal machinery of sleep homeostasis in Drosophila. Neuron 2014;81. https://doi.org/10.1016/j.neuron.2013.12.013.

[24] Kempf A, Song SM, Talbot CB, Miesenböck G. A potassium channel β-subunit couples mitochondrial electron transport to sleep. Nature 2019;568. https://doi.org/10.1038/s41586-019-1034-5.

[25] Aso Y, Sitaraman D, Ichinose T, Kaun KR, Vogt K, Belliart-Guérin G, et al. Mushroom body output neurons encode valence and guide memory-based action selection in Drosophila. Elife 2014;3. https://doi.org/10.7554/eLife.04580.

[26] Joiner WJ, Crocker A, White BH, Sehgal A. Sleep in Drosophila is regulated by adult mushroom bodies. Nature 2006;441. https://doi.org/10.1038/nature04811.

[27] Blum ID, Keleş MF, Baz ES, Han E, Park K, Luu S, et al. Astroglial Calcium Signaling Encodes Sleep Need in Drosophila. Current Biology 2021;31. https://doi.org/10.1016/j.cub.2020.10.012.

[28] Liu S, Lamaze A, Liu Q, Tabuchi M, Yang Y, Fowler M, et al. WIDE AWAKE mediates the circadian timing of sleep onset. Neuron 2014;82:151–66. https://doi.org/10.1016/j.neuron.2014.01.040.

[29] Blum ID, Bell B, Wu MN. Time for Bed: Genetic Mechanisms Mediating the Circadian Regulation of Sleep. Trends in Genetics 2018;34. https://doi.org/10.1016/j.tig.2018.01.001.

[30] Shaw P, Cirelli C, Greenspan R, Tononi G. Correlates of sleep and waking in Drosophila melanogaster. Science 2000;287:1834–7. https://doi.org/10.1126/SCIENCE.287.5459.1834.

[31] Borbély AA, Schneider D. Secrets of sleep 1986:228.

[32] Shaw PJ, Franken P. Perchance to dream: solving the mystery of sleep through genetic analysis. J Neurobiol 2003;54:179–202. https://doi.org/10.1002/NEU.10167.

[33] Stahl BA, Slocumb ME, Chaitin H, DiAngelo JR, Keene AC. Sleep-dependent modulation of metabolic rate in drosophila. Sleep 2017;40. https://doi.org/10.1093/sleep/zsx084.

[34] van Alphen B, Yap MHW, Kirszenblat L, Kottler B, van Swinderen B. A dynamic deep sleep stage in Drosophila. Journal of Neuroscience 2013;33. https://doi.org/10.1523/JNEUROSCI.0061-13.2013.

[35] Yap MHW, Grabowska MJ, Rohrscheib C, Jeans R, Troup M, Paulk AC, et al. Oscillatory brain activity in spontaneous and induced sleep stages in flies. Nat Commun 2017;8. https://doi.org/10.1038/s41467-017-02024-y.

[36] Xu X, Yang W, Tian B, Sui X, Chi W, Rao Y, et al. Quantitative investigation reveals distinct phases in Drosophila sleep. Commun Biol 2021;4. https://doi.org/10.1038/s42003-021-01883-y.

[37] Wiggin TD, Goodwin PR, Donelson NC, Liu C, Trinh K, Sanyal S, et al. Covert sleep-related biological processes are revealed by probabilistic analysis in Drosophila. Proc Natl Acad Sci U S A 2020;117. https://doi.org/10.1073/pnas.1917573117.

[38] Tainton-Heap LAL, Kirszenblat LC, Notaras ET, Grabowska MJ, Jeans R, Feng K, et al. A Paradoxical Kind of Sleep in Drosophila melanogaster. Current Biology 2021;31. https://doi.org/10.1016/j.cub.2020.10.081.

[39] Raccuglia D, Huang S, Ender A, Heim MM, Laber D, Suárez-Grimalt R, et al. Network-Specific Synchronization of Electrical Slow-Wave Oscillations Regulates Sleep Drive in Drosophila. Current Biology 2019;29. https://doi.org/10.1016/j.cub.2019.08.070.

[40] Abhilash L. phase: Analyse Biological Time-Series Data 2021.

[41] Refinetti R, Cornélissen G, Halberg F. Procedures for numerical analysis of circadian rhythms. Biol Rhythm Res 2007;38:275–325. https://doi.org/10.1080/09291010600903692.

[42] Ruf T. The Lomb-Scargle periodogram in biological rhythm research: Analysis of incomplete and unequally spaced time-series. Biol Rhythm Res 1999;30. https://doi.org/10.1076/brhm.30.2.178.1422.

[43] Brown LA, Fisk AS, Pothecary CA, Peirson SN. Telling the time with a broken clock: Quantifying circadian disruption in animal models. Biology (Basel) 2019;8. https://doi.org/10.3390/biology8010018.

[44] Tackenberg MC, Hughey JJ. The risks of using the chi-square periodogram to estimate the period of biological rhythms. PLoS Comput Biol 2021;17. https://doi.org/10.1371/JOURNAL.PCBI.1008567.

[45] Lack LC, Lushington K. The rhythms of human sleep propensity and core body temperature. J Sleep Res 1996;5:1–11. https://doi.org/10.1046/J.1365-2869.1996.00005.X.

[46] Huber R, Deboer T, Tobler I. Effects of sleep deprivation on sleep and sleep EEG in three mouse strains: Empirical data and simulations. Brain Res 2000;857. https://doi.org/10.1016/S0006-8993(99)02248-9.

[47] Dowse HB, Hall JC, Ringo JM. Circadian and ultradian rhythms in period mutants of Drosophila melanogaster. Behav Genet 1987;17. https://doi.org/10.1007/BF01066008.

[48] Seki Y, Tanimura T. Ultradian rhythm unmasked in the Pdf clock mutant of Drosophila. J Biosci 2014;39. https://doi.org/10.1007/s12038-014-9450-z.

[49] Leise TL. Wavelet analysis of circadian and ultradian behavioral rhythms. J Circadian Rhythms 2013;11:5. https://doi.org/10.1186/1740-3391-11-5.
[50] Brancaccio M, Edwards MD, Patton AP, Smyllie NJ, Chesham JE, Maywood ES, et al. Cell-autonomous clock of astrocytes drives circadian behavior in mammals. Science (1979) 2019;363. https://doi.org/10.1126/science.aat4104.
[51] Leise TL. Analysis of Nonstationary Time Series for Biological Rhythms Research: Http://DxDoiOrg/101177/0748730417709105 2017;32:187–94. https://doi.org/10.1177/0748730417709105.
[52] Price TS, Baggs JE, Curtis AM, Fitzgerald GA, Hogenesch JB. WAVECLOCK: wavelet analysis of circadian oscillation. Bioinformatics 2008;24:2794–5. https://doi.org/10.1093/BIOINFORMATICS/BTN521.
[53] Leise TL, Harrington ME. Wavelet-based time series analysis of Circadian rhythms. J Biol Rhythms 2011;26. https://doi.org/10.1177/0748730411416330.
[54] Dowse HB, Ringo JM. Further Evidence that the Circadian Clock in Drosophila is a Population of Coupled Ultradian Oscillators. J Biol Rhythms 1987;2. https://doi.org/10.1177/074873048700200106.
[55] Tobler I, Borbély AA, Groos G. The effect of sleep deprivation on sleep in rats with suprachiasmatic lesions. Neurosci Lett 1983;42. https://doi.org/10.1016/0304-3940(83)90420-2.
[56] Wisor JP, O'Hara BF, Terao A, Selby CP, Kilduff TS, Sancar A, et al. A role of cryptochromes in sleep regulation. BMC Neurosci 2002;3. https://doi.org/10.1186/1471-2202-3-20.
[57] Larkin JE, Yokogawa T, Heller HC, Franken P, Ruby NF. Homeostatic regulation of sleep in arrhythmic Siberian hamsters. Am J Physiol Regul Integr Comp Physiol 2004;287. https://doi.org/10.1152/ajpregu.00676.2003.
[58] Trachsel L, Edgar DM, Seidel WF, Craig Heller H. Sleep homeostasis in suprachiasmatic nuclei-lesioned rats: effects of sleep deprivation and triazolam administration. Brain Res 1992;589:253–61. https://doi.org/10.1016/0006-8993(92)91284-L.
[59] Naylor E, Bergmann BM, Krauski K, Zee PC, Takahashi JS, Vitaterna MH, et al. The circadian Clock mutation alters sleep homeostasis in the mouse. Journal of Neuroscience 2000;20. https://doi.org/10.1523/jneurosci.20-21-08138.2000.
[60] Franken P, Thomason R, Craig HC, O'Hara BF. A non-circadian role for clock-genes in sleep homeostasis: A strain comparison. BMC Neurosci 2007;8. https://doi.org/10.1186/1471-2202-8-87.
[61] Laposky A, Easton A, Dugovic C, Walisser J, Bradfield C, Turek F. Deletion of the mammalian circadian clock gene BMAL1/Mop3 alters baseline sleep architecture and the response to sleep deprivation. Sleep 2005;28. https://doi.org/10.1093/sleep/28.4.395.
[62] Shaw PJ, Tortoni G, Greenspan RJ, Robinson DF. Stress response genes protect against lethal effects of sleep deprivation in Drosophila. Nature 2002;417. https://doi.org/10.1038/417287a.

[63] Shiromani PJ, Xu M, Winston EM, Shiromani SN, Gerashchenko D, Weaver DR. Sleep rhythmicity and homeostasis in mice with targeted disruption of mPeriod genes. Am J Physiol Regul Integr Comp Physiol 2004;287. https://doi.org/10.1152/ajpregu.00138.2004.

[64] Dijk DJ, Archer SN. PERIOD3, circadian phenotypes, and sleep homeostasis. Sleep Med Rev 2010;14. https://doi.org/10.1016/j.smrv.2009.07.002.

[65] Konopka RJ, Hamblen-Coyle MJ, Jamison CF, Hall JC. An Ultrashort Clock Mutation at the period Locus of Drosophila melanogaster That Reveals Some New Features of the Fly's Circadian System. J Biol Rhythms 1994;9. https://doi.org/10.1177/074873049400900303.

[66] Konopka RJ, Benzer S. Clock Mutants of Drosophila melanogaster. Proceedings of the National Academy of Sciences 1971;68:2112–6. https://doi.org/10.1073/pnas.68.9.2112.

[67] Hoofdakker R, van Den H, Bos KHN, van den Burg W. In search of a depressive sleep syndrome. In: van Praag HM, Meinardi H, editors. Brain and Sleep, Amsterdam: Bohn: 1974.

[68] Franken P, Dijk DJ, Tobler I, Borbely AA. Sleep deprivation in rats: Effects on EEG power spectra, vigilance states, and cortical temperature. Am J Physiol Regul Integr Comp Physiol 1991;261. https://doi.org/10.1152/ajpregu.1991.261.1.r198.

[69] Emery P, Stanewsky R, Helfrich-Förster C, Emery-Le M, Hall JC, Rosbash M. Drosophila CRY Is a Deep Brain Circadian Photoreceptor. Neuron 2000;26:493–504. https://doi.org/10.1016/S0896-6273(00)81181-2.

[70] Stanewsky R, Kaneko M, Emery P, Beretta B, Wager-Smith K, Kay SA, et al. The cryb Mutation Identifies Cryptochrome as a Circadian Photoreceptor in Drosophila. Cell 1998;95:681–92. https://doi.org/10.1016/S0092-8674(00)81638-4.

[71] Hunter-Ensor M, Ousley A, Sehgal A. Regulation of the Drosophila protein timeless suggests a mechanism for resetting the circadian clock by light. Cell 1996;84. https://doi.org/10.1016/S0092-8674(00)81046-6.

[72] Riggle JP, Kay LM, Onishi KG, Falk DT, Smarr BL, Zucker I, et al. Modified Wavelet Analyses Permit Quantification of Dynamic Interactions Between Ultradian and Circadian Rhythms. J Biol Rhythms 2022;37:631–54. https://doi.org/10.1177/07487304221128652.

[73] Persons JL, Abhilash L, Lopatkin AJ, Roelofs A, Bell E v, Fernandez MP, et al. PHASE: An Open-Source Program for the Analysis of DrosophilaPhase, Activity, and Sleep Under Entrainment. J Biol Rhythms 2022;37:455–67. https://doi.org/10.1177/07487304221093114.

[74] Achermann P, Borbély AA. Simulation of Human Sleep: Ultradian Dynamics of Electroencephalographic Slow-Wave Activity. J Biol Rhythms 1990;5. https://doi.org/10.1177/074873049000500206.

[75] ACHERMANN P, BORBÉLY AA. Combining different models of sleep regulation. J Sleep Res 1992;1. https://doi.org/10.1111/j.1365-2869.1992.tb00028.x.

[76] Achermann P, Dijk DJ, Brunner DP, Borbély AA. A model of human sleep homeostasis based on EEG slow-wave activity: Quantitative comparison of data and simulations. Brain Res Bull 1993;31. https://doi.org/10.1016/0361-9230(93)90016-5.

[77] Mistlberger RE, Bergmann BM, Waldenar W, Rechtschaffen A. Recovery sleep following sleep deprivation in intact and suprachiasmatic nuclei-lesioned rats. Sleep 1983;6. https://doi.org/10.1093/sleep/6.3.217.

[78] Dowse HB, Ringo JM. Do Ultradian Oscillators Underlie the Circadian Clock in Drosophila? Ultradian Rhythms in Life Processes, 1992. https://doi.org/10.1007/978-1-4471-1969-2_6.

[79] Dijk DJ, Beersma DGM, Daan S. EEG Power Density during Nap Sleep: Reflection of an Hourglass Measuring the Duration of Prior Wakefulness. J Biol Rhythms 1987;2. https://doi.org/10.1177/074873048700200304.

[80] Marrus SB, Zeng H, Rosbash M. Effect of constant light and circadian entrainment of perS flies: evidence for light-mediated delay of the negative feedback loop in Drosophila. EMBO J 1996;15:6877. https://doi.org/10.1002/j.1460-2075.1996.tb01080.x.

[81] Li Y, Shan Y, Kilaru G, Berto S, Wang GZ, Cox KH, et al. Epigenetic inheritance of circadian period in clonal cells. Elife 2020;9. https://doi.org/10.7554/eLife.54186.

[82] Nikhil KL, Korge S, Kramer A. Heritable gene expression variability and stochasticity govern clonal heterogeneity in circadian period. PLoS Biol 2020;18. https://doi.org/10.1371/JOURNAL.PBIO.3000792.

[83] Viola AU, Archer SN, James LMM, Groeger JA, Lo JCY, Skene DJ, et al. PER3 Polymorphism Predicts Sleep Structure and Waking Performance. Current Biology 2007;17. https://doi.org/10.1016/j.cub.2007.01.073.

[84] Franken P, Tobler I, Borbély AA. Sleep homeostasis in the rat: Simulation of the time course of EEG slow-wave activity. Neurosci Lett 1991;130. https://doi.org/10.1016/0304-3940(91)90382-4.

[85] Schwartz WJ, Zimmerman P. Circadian timekeeping in BALB/c and C57BL/6 inbred mouse strains. Journal of Neuroscience 1990;10. https://doi.org/10.1523/jneurosci.10-11-03685.1990.

[86] Czeisler CA, Duffy JF, Shanahan TL, Brown EN, Mitchell JF, Rimmer DW, et al. Stability, precision, and near-24-hour period of the human circadian pacemaker. Science (1979) 1999;284. https://doi.org/10.1126/science.284.5423.2177.

[87] Liang X, Holy TE, Taghert PH. Synchronous drosophila circadian pacemakers display nonsynchronous Ca2+ rhythms in vivo. Science (1979) 2016;351. https://doi.org/10.1126/science.aad3997.

[88] Lamaze A, Krätschmer P, Chen KF, Lowe S, Jepson JEC. A Wake-Promoting Circadian Output Circuit in Drosophila. Current Biology 2018;28. https://doi.org/10.1016/j.cub.2018.07.024.

[89] Kunst M, Hughes ME, Raccuglia D, Felix M, Li M, Barnett G, et al. Calcitonin gene-related peptide neurons mediate sleep-specific circadian output in Drosophila. Current Biology 2014;24. https://doi.org/10.1016/j.cub.2014.09.077.

[90] Guo F, Holla M, Díaz MM, Rosbash M. A Circadian Output Circuit Controls Sleep-Wake Arousal in Drosophila. Neuron 2018;100. https://doi.org/10.1016/j.neuron.2018.09.002.

[91] Guo F, Yu J, Jung HJ, Abruzzi KC, Luo W, Griffith LC, et al. Circadian neuron feedback controls the Drosophila sleep-activity profile. Nature 2016;536. https://doi.org/10.1038/nature19097.

[92] Barber AF, Erion R, Holmes TC, Sehgal A. Circadian and feeding cues integrate to drive rhythms of physiology in Drosophila insulin-producing cells. Genes Dev 2016;30. https://doi.org/10.1101/gad.288258.116.

[93] Roesch A, Schmidbauer H. WaveletComp: Computational Wavelet Analysis 2018.

[94] Aldrich E. wavelets: Functions for Computing Wavelet Filters, Wavelet Transforms and Multiresolution Analyses 2020.

[95] Kohl M. MKinfer: Inferential Statistics 2022.

[96] Geissmann Q, Beckwith EJ, Gilestro GF. Most sleep does not serve a vital function: Evidence from Drosophila melanogaster. Sci Adv 2019;5. https://doi.org/10.1126/SCIADV.AAU9253.

[97] Ram K, Wickham H. wesanderson: A Wes Anderson Palette Generator 2018.

1024 ## Figure Legends

1025

1026 **Figure 1: Circadian analysis of *Drosophila* sleep.** (A) A schematic of a two-process model that
1027 leads to one episode of sleep/cycle. (B) Somnograms (left) and actograms (right) of *Canton-S*
1028 (*CS*; top), w^{1118} (middle), and *yw* (bottom) flies under light/dark 12:12 (LD12:12) cycles and
1029 constant darkness (DD). Gray shaded regions indicate the dark phase of the LD cycle.
1030 Representative Chi-square periodograms of sleep time-series (C) under LD12:12 (top) and DD
1031 (bottom), and of locomotor activity time-series (D) under LD12:12 (top) and DD (bottom) of the
1032 three genotypes of flies. The red lines indicate the Chi-square significance line at $\alpha = 0.05$. Height
1033 of peaks of the black lines indicate the strength of that periodicity in the time-series. (E) Frequency
1034 distributions of percentage time spent sleeping/24-h cycle in the three genotypes under LD12:12.

1035

1036 **Figure 2: Building a *Drosophila* two-process model of sleep regulation.** (A) Heatmap
1037 summarizing the nature of sleep rhythms within the build-up and decay time constant parameter
1038 space for sleep pressure. (B) Heatmap showing the sum of squared differences (SSD) between
1039 model prediction and empirical values in the same parameter space for the value combinations
1040 producing bi-episodic/bimodal rhythms. The red lines along the *x*- and *y*-axes represent the sleep
1041 pressure parameters that best fit empirical data. (C) The two-process model with best-fitting
1042 parameters describing fly sleep. (D) The percentage of time spent sleeping/24-cycle in the three
1043 genotypes and their average value compared with the predicted value from the model.

1044

1045 **Figure 3: Ultradian periodicities are a predictable consequence of a functional S-process**
1046 **under a dysfunctional C-process.** (A) The wildtype two-process model (top) and the somnogram

of simulated sleep data produced by this model (bottom). (B) The same model as in panel (A) but with flat, non-oscillating thresholds to model sleep regulation in a loss-of-function clock mutant (top) and the somnogram it produced (bottom). (C) Four representative continuous wavelet transform (CWT) scalograms for *Canton-S* (*CS*; C) and (D) one each for per^{01}, tim^{01}, clk^{JRK} and cyc^{01}. The color bars against each scalogram are representative of local rhythmic power. Note: the *y*-axes on the scalograms are on a logarithmic scale, and the data are binned in 60-min intervals. (E) Wavelet detail-specific characterization of sleep/wake rhythms (binned in 1-min intervals) show the % energy at each scale. Details 5 and 6 correspond to ultradian periods ranging from 32-min to 2-h. Detail 10 corresponds to the circadian range (17- to 34-h). The wildtype data set is replotted in each panel to facilitate comparisons with the four mutant lines. Values plotted are mean±SEM. See text for details. For each detail level, two-sample t-tests were carried out for comparing wildtype and mutant flies, which would result in 10 overall comparisons. The *p*-values reported were adjusted for multiple comparisons, using a Benjamini-Hochberg correction. Statistical results are shown only for details 5 (per^{01} *vs CS*: $t_{56.02} = -10.85$, $p = 2.15e-14$; tim^{01} *vs CS*: $t_{49.07} = -8.69$, $p = 1.69e-10$; clk^{JRK} *vs CS*: $t_{56.66} = -4.36$, $p = 0.0001$; cyc^{01} *vs CS*: $t_{61.04} = -6.53$, $p = 1.45e-07$), 6 (per^{01} *vs CS*: $t_{53.14} = -5.08$, $p = 9.87e-06$; tim^{01} *vs CS*: $t_{55.05} = -3.42$, $p = 0.002$; clk^{JRK} *vs CS*: $t_{61.98} = -5.06$, $p = 1.35e-05$; cyc^{01} *vs CS*: $t_{50.95} = -6.03$, $p = 6.12e-07$) and 10 (per^{01} *vs CS*: $t_{34.95} = 6.58$, $p = 6.76e-07$; tim^{01} *vs CS*: $t_{34.12} = 6.68$, $p = 5.57e-07$; clk^{JRK} *vs CS*: $t_{34.27} = 5.92$, $p = 7.66e-06$; cyc^{01} *vs CS*: $t_{58.66} = 3.21$, $p = 0.003$). * < 0.05, ** < 0.01, *** < 0.001, **** < 0.0001, and N.S. (Not Significant).

Figure 4: The model predicts regions of relatively weak sleep rhythms across a range of free-running periods which do not match empirical data. (A) Schematic representation of the

1070 simulation workflow upon which predictions were made. (B) Power of sleep rhythms and (C)
1071 time spent sleeping/circadian cycle for flies with different free-running periods, generated through
1072 combinations of five *period* alleles (see Materials and Methods). (D) Median power of sleep
1073 rhythms (mean±SEM across two replicate runs) and (E) time spent sleeping/circadian cycle
1074 (mean±SEM across two replicate runs) across the entire range of free-running periods overlayed
1075 with the predictions of the two-process model when only the free-running period was altered in
1076 the model.
1077
1078 **Figure 5: Allowing homeostatic parameters to change with free-running periods suggest a**
1079 **strong inter-dependence between the S- and C-processes.** (A) Schematic representation of the
1080 simulation routine to estimate best fitting S-process parameters for each individual fly. (B) Median
1081 power of sleep rhythms (mean±SEM across two replicate runs) and (C) time spent
1082 sleeping/circadian cycle (mean±SEM across two replicate runs) across the entire range of free-
1083 running periods overlayed with the predictions of the two-process model when build-up and decay
1084 time constants were allowed to covary with the free-running period. Note that the experimental
1085 data shown in panels (B) and (C) are the same as those shown in Figs. 4D and 4E and have been
1086 replotted here to facilitate comparisons. (D) The relationship between build-up time constant (left)
1087 and decay time constant (right) of sleep pressure and free-running periods. Values plotted are
1088 mean±SEM. The red solid line is the estimate from a linear regression model and the dotted red
1089 lines are the 95% confidence intervals. Also shown are the regions along the *x*-axis corresponding
1090 to the free-running periods of males bearing the four rhythmic *period* alleles used in our study (see
1091 also Table 2).
1092

1093 **Figure 6: Short bout sleep is dispensable for capturing the relationship between circadian**
1094 **period and amount of sleep.** (A) Scatter plots of the amount of time spent sleeping/circadian
1095 minute across different free-running periods for different inactivity duration-based definitions of
1096 sleep overlayed with the amounts of sleep measured using standard definition of sleep and the
1097 amounts predicted by the model. All the sleep amounts are scaled to maxima so as to restrict the
1098 *y*-axis between 0 and 1. Note that the same model and standard definition of sleep data are re-
1099 plotted in every panel to facilitate comparisons. For each definition of sleep (shown in red), the *y*-
1100 axis is plotted on the right side of the plot. In case of the bottom three panels, the minima values
1101 on the secondary *y*-axis (in red) have been adjusted to enable easy visual comparisons. Note that
1102 data for the amount of sleep using the 5-min definition of sleep are the same as that depicted in
1103 Figs. 4E and 5C. Each dot in all the panels represents the median value of flies within each detected
1104 free-running period, averaged over two independent replicate runs. (B) The correlation
1105 coefficients from Pearson's product-moment correlations on the raw amounts of sleep/circadian
1106 cycle between model predictions and different inactivity duration-based definitions of sleep. The
1107 scaling of data and adjustment of the *y*-axis have no bearing on the correlation coefficients
1108 reported.
1109
1110 **Figure 7: Independent tests confirm the relationship between free-running period and the**
1111 **rates of change of sleep homeostat.** (A) Schematic representation of the predictions for short
1112 period flies having altered sleep homeostatic parameters. (B) Time-series of long bout sleep of
1113 both genotypes under continuous white light for 15 days. Discrete wavelet transform based
1114 estimate of scale-wise concentration of spectral variance in (C) *CS* and (D) per^S flies (also see
1115 Materials and Methods). Shown are mean estimates of % energy±SEM. Note the three period

1116 bands that comprise maximal spectral energy. (E) Ultradian periods (mean±SEM) for the two
1117 genotypes under LL as estimated from the continuous wavelet transforms (Results based on one-
1118 tailed bootstrapped Welch two-sample *t*-tests – τ_s: $t_{30.72} = 2.49$, $p = 0.004$; τ_m: $t_{29.46} = 0.57$, $p =$
1119 0.30; τ_i: $t_{35.58} = -1.19$, $p = 0.88$). (F) Boxplots of total sleep over 15 cycles ($W = 860$; $p = 4.18e-$
1120 07) and (G) of total number of long bout sleep episodes over 15 cycles ($W = 264.5$; $p = 0.0005$)
1121 show significant differences in the direction predicted by the model. Statistical comparisons were
1122 made using the one-tailed Wilcoxon's test. * < 0.05, ** < 0.01, *** < 0.001, **** < 0.0001, and
1123 N.S. (Not Significant).
1124
1125 **Figure 8: Utility of the two-process model in generating testable predictions.** (A) Predicted
1126 roles played by the rising and falling phases of the thresholds in regulating the timing and
1127 maintenance of sleep, in the context of the two-process model. Hypothetical relationships between
1128 Ca^{2+} levels in circadian clock neurons, the two-process model, and sleep behavior. Data for the
1129 Ca^{2+} levels were extracted from Liang et al., 2016 [87] and smoothed using custom R scripts.
1130 Light gray shaded regions represent the subjective day phase, and the dark gray shaded regions
1131 represent the subjective night phase of one circadian cycle. The number of arrowheads is
1132 representative of the hypothesized strength of effects of calcium activity on the upper and lower
1133 thresholds, respectively. (B) A schematic representation of the effect of activation of DN-1s on
1134 sleep behavior previously reported by others. Exciting DN-1ps is predicted to produce an earlier
1135 fall and prolonged suppression of the lower threshold oscillations (dotted green lines). As a
1136 consequence of the earlier falling of the threshold, sleep pressure takes longer to hit the lower
1137 threshold (dotted red line) thereby increasing daytime sleep as was observed in two previous
1138 studies (bottom panel). The plots in the bottom panel are redrawn from Guo et al. (2016) [91] and

1139 Kunst et al. (2014) [89]. Green lines represent sleep in the DN-1p activated flies and the black
1140 lines represent unmanipulated controls. This manipulation also leads to an earlier termination of
1141 nighttime sleep as was reported by Kunst et al., (2014) [89], which is also explained by the effect
1142 of exciting DN-1ps on the lower threshold of the two-process model. (C) Two-process models
1143 and associated somnograms under unchanged conditions (left) and conditions of complete loss of
1144 decrease in the lower threshold (right). The complete loss of decrease in the lower threshold below
1145 baseline is taken to mimic a condition of inhibited DNs. Note the clear case of disrupted
1146 sleep/wake rhythms under constant darkness in this situation as compared to the wildtype situation
1147 (left). It is important to note that our specific quantitative predictions of sleep rhythms are
1148 produced by the best-fitting parameters of build-up and decay time constants derived from
1149 wildtype flies.
1150

1151 # Tables

1152 **Table 1:** Adjusted power values (mean±SEM) of *Canton-S* (*CS*), w^{1118} and *yw* flies from Chi-
1153 square periodogram analyses on sleep and locomotor activity time-series under LD and DD
1154 conditions in the circadian range (between 16- to 32-h). Also reported are the differences in power
1155 values between sleep and locomotor activity powers for each genotype. Sample sizes are provided
1156 in parentheses.

	CS		***w^{1118}***		***yw***	
	LD12:12	**DD**	**LD12:12**	**DD**	**LD12:12**	**DD**
Sleep	4006.7 ± 163.0 (32)	2119.6 ± 242.1 (31)	3964.3 ± 138.1 (31)	3107.3 ± 200.7 (31)	3022.8 ± 211.1 (31)	1613.0 ± 140.5 (28)
Locomotor activity	1345.3 ± 180.5 (32)	503.8 ± 89.3 (28)	2657.2 ± 125.6 (31)	1200.2 ± 110.1 (31)	638.8 ± 120.7 (30)	296.2 ± 60.7 (27)
Δ Power	2661.4	1615.8	1307.1	1907.2	2384.0	1316.8

1157
1158

1159 **Table 2:** Median free-running periods of sleep rhythms under constant darkness averaged across

1160 two replicate runs. The values for male (top, blue) and female (bottom, red) progeny from each

1161 cross are reported. Outcomes of any cross that had fewer than 12 flies pooled from both replicate

1162 runs have not been reported in this table. Sample sizes are provided in parentheses.

Paternal genotype	Maternal genotype: per^T	per^S	per^+	per^L	per^{01}
per^T	♂: 15.25 (44) ♀: 17.75 (38)	♂: 19.75 (30) ♀: 18.50 (24)	♂: 24.25 (63) ♀: 20.50 (55)	♂: 28.75 (62) ♀: 21.75 (55)	♂: NA ♀: 19.75 (60)
per^S	♂: 17.00 (63) ♀: 19.25 (59)	♂: 21.00 (34) ♀: 20.38 (12)	♂: 24.25 (59) ♀: 22.00 (53)	♂: 28.25 (60) ♀: 23.50 (62)	♂: NA ♀: 21.50 (56)
per^+	♂: 16.25 (51) ♀: 20.75 (59)	♂: 19.63 (60) ♀: 22.00 (62)	♂: 23.50 (47) ♀: 24.00 (57)	♂: 27.50 (59) ♀: 24.75 (63)	♂: NA ♀: 25.00 (63)
per^L	♂: 16.50 (30) ♀: 22.00 (31)	♂: 20.00 (61) ♀: 23.00 (55)	♂: 24.00 (59) ♀: 24.50 (63)	♂: 27.75 (42) ♀: 27.50 (53)	♂: NA ♀: 29.75 (55)
per^{01}	♂: NA ♀: NA	♂: 20.00 (29) ♀: 21.50 (28)	♂: 24.25 (47) ♀: 25.00 (57)	♂: 28.50 (60) ♀: 29.50 (55)	♂: NA ♀: NA

1163

1164

1165 **Table 3:** Median Chi-square periodogram power of sleep rhythms under constant darkness
1166 averaged across two replicate runs. The values for male (top, blue) and female (bottom, red)
1167 progeny from each cross are reported. Outcomes of any cross that had fewer than 12 flies pooled
1168 from the replicate runs have not been reported in this table. Sample sizes are provided in
1169 parentheses.

Paternal genotype	Maternal genotype: per^T	per^S	per^+	per^L	per^{01}
per^T	♂: 33.0 (44) ♀: 33.6 (38)	♂: 187.5 (30) ♀: 143.9 (24)	♂: 136.1 (63) ♀: 79.5 (55)	♂: 135.5 (62) ♀: 98.4 (55)	♂: NA ♀: 119.4 (60)
per^S	♂: 98.0 (63) ♀: 110.7 (59)	♂: 109.7 (34) ♀: 40.7 (12)	♂: 95.9 (59) ♀: 105.1 (53)	♂: 137.5 (60) ♀: 70.8 (62)	♂: NA ♀: 103.3 (56)
per^+	♂: 51.5 (51) ♀: 76.4 (59)	♂: 161.0 (60) ♀: 117.0 (62)	♂: 79.4 (47) ♀: 92.6 (57)	♂: 64.9 (59) ♀: 118.0 (63)	♂: NA ♀: 130.3 (63)
per^L	♂: 93.7 (30) ♀: 108.4 (31)	♂: 81.1 (61) ♀: 55.5 (55)	♂: 53.9 (59) ♀: 134.0 (63)	♂: 72.0 (42) ♀: 85.4 (53)	♂: NA ♀: 92.8 (55)
per^{01}	♂: NA ♀: NA	♂: 114.6 (29) ♀: 114.4 (28)	♂: 32.7 (47) ♀: 102.4 (57)	♂: 56.1 (60) ♀: 72.7 (55)	♂: NA ♀: NA

1170

1171

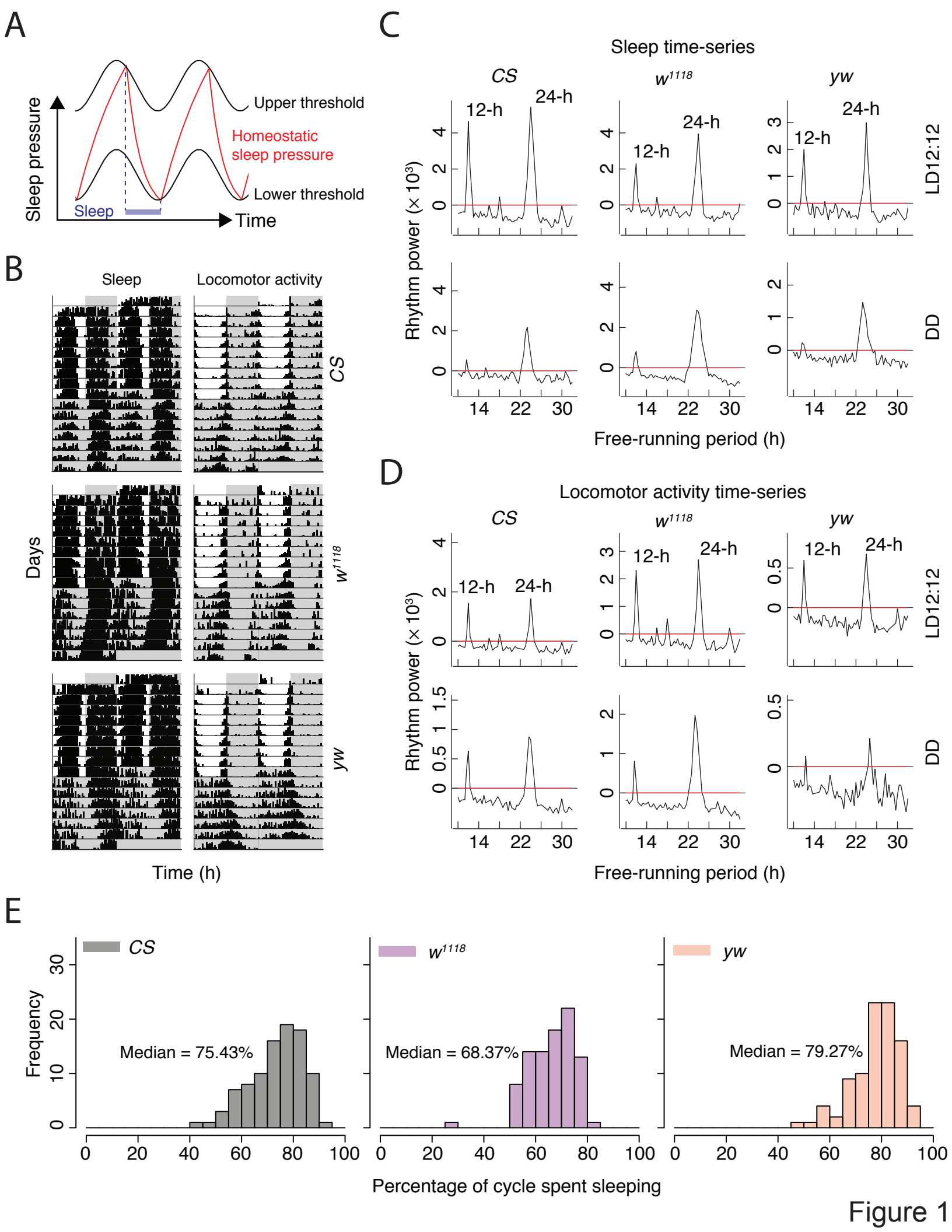
A
Sleep pressure
Upper threshold
Homeostatic sleep pressure
Lower threshold
Sleep
Time
B
Sleep
Locomotor activity
CS
w1118
yw
Days
Time (h)
C
Sleep time-series
CS
w1118
yw
12-h
24-h
LD12:12
DD
Rhythm power (× 10³)
Free-running period (h)
D
Locomotor activity time-series
CS
w1118
yw
12-h
24-h
LD12:12
DD
Rhythm power (× 10³)
Free-running period (h)
E
CS
w1118
yw
Frequency
Median = 75.43%
Median = 68.37%
Median = 79.27%
Percentage of cycle spent sleeping

Figure 1

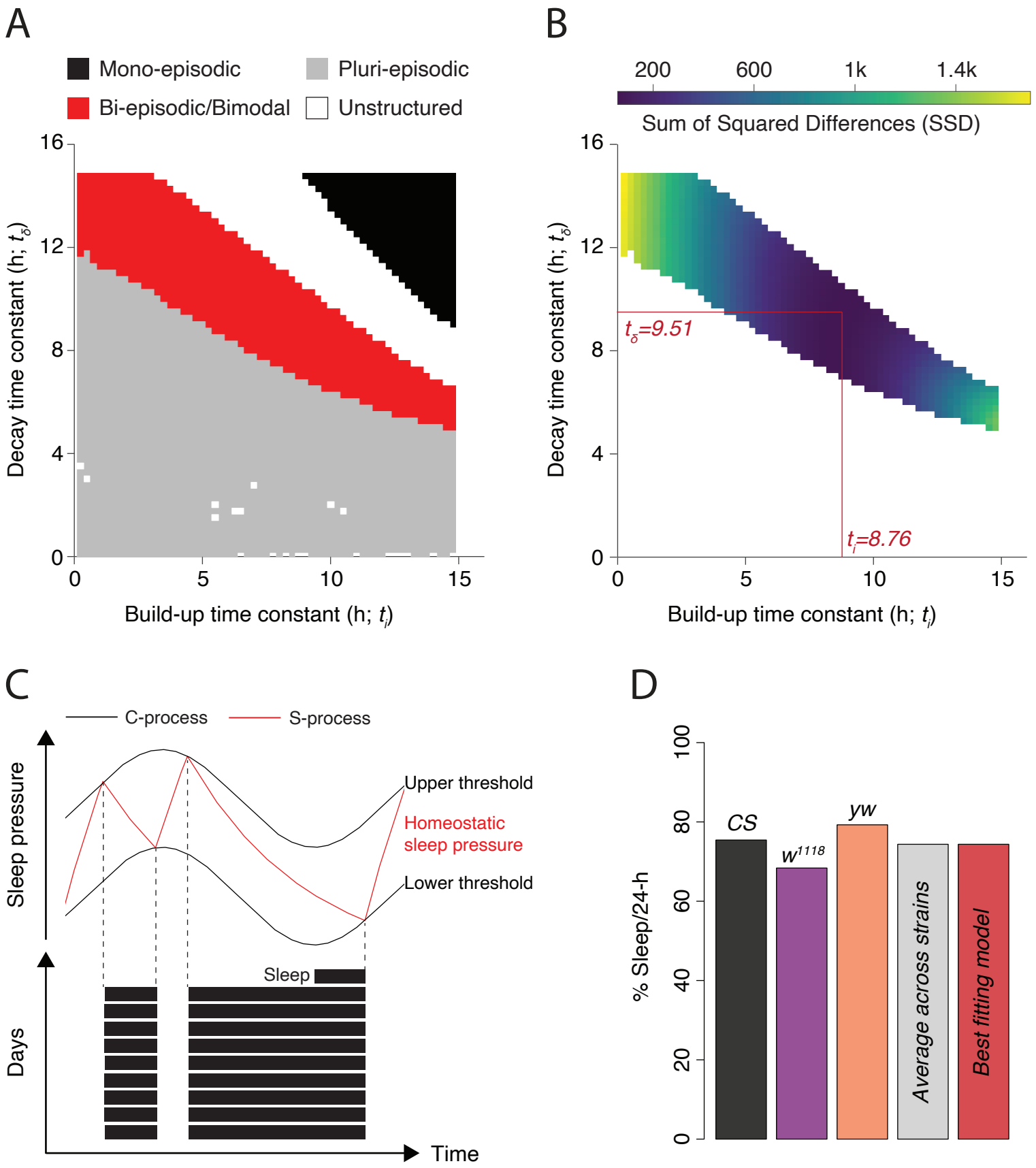
A
Mono-episodic
Pluri-episodic
Bi-episodic/Bimodal
Unstructured
Decay time constant (h; t_δ)
Build-up time constant (h; t_i)
B
200
600
1k
1.4k
Sum of Squared Differences (SSD)
t_δ=9.51
t_i=8.76
C
C-process
S-process
Sleep pressure
Upper threshold
Homeostatic sleep pressure
Lower threshold
Sleep
Days
Time
D
% Sleep/24-h
CS
w^{1118}
yw
Average across strains
Best fitting model

Figure 2

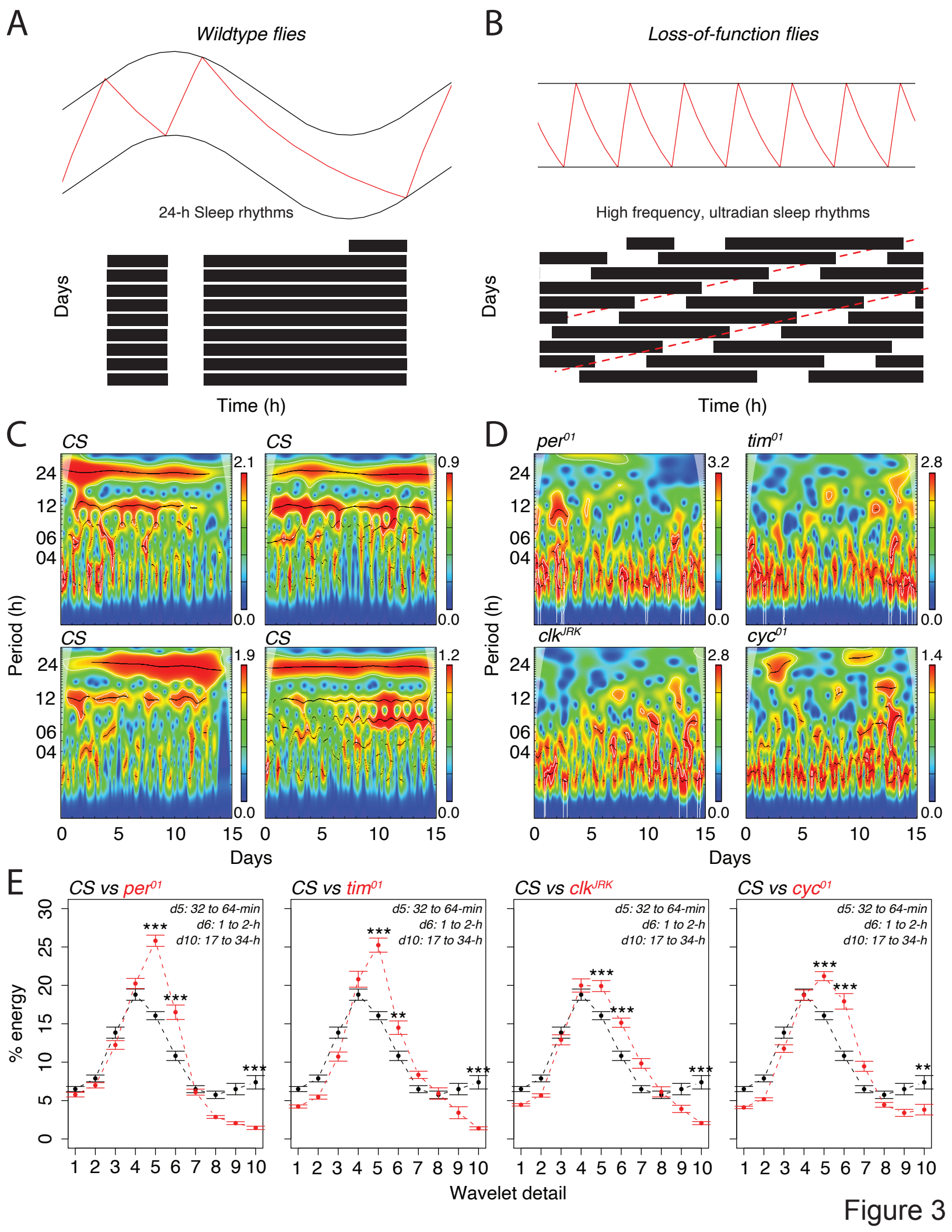
A
Wildtype flies
24-h Sleep rhythms
Days
Time (h)
B
Loss-of-function flies
High frequency, ultradian sleep rhythms
Days
Time (h)
C
CS
CS
CS
CS
Period (h)
Days
D
per01
tim01
clkJRK
cyc01
Period (h)
Days
E
CS vs per01
CS vs tim01
CS vs clkJRK
CS vs cyc01
d5: 32 to 64-min
d6: 1 to 2-h
d10: 17 to 34-h
% energy
Wavelet detail

Figure 3

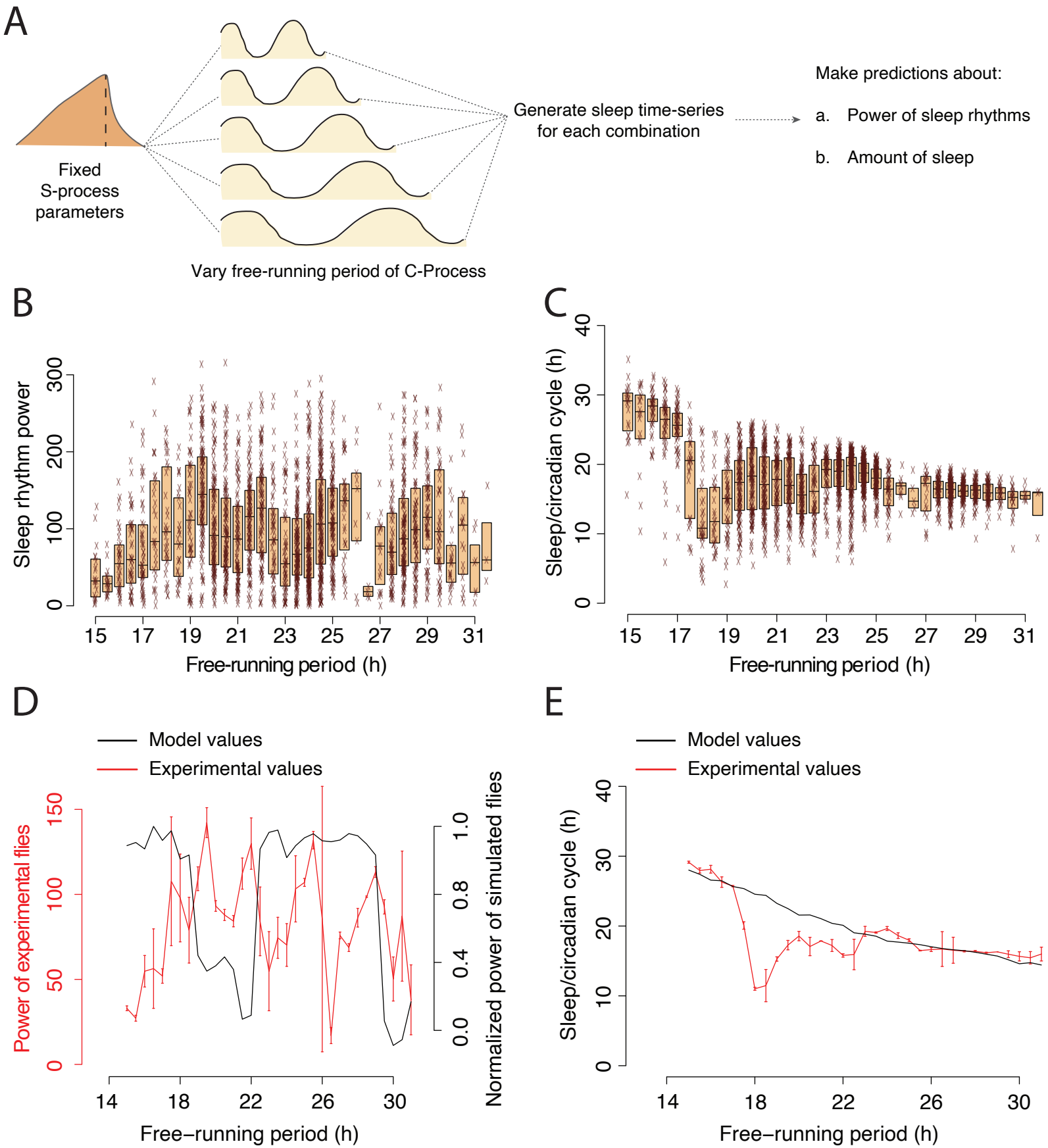
A
Fixed
S-process
parameters
Vary free-running period of C-Process
Generate sleep time-series
for each combination
Make predictions about:
a. Power of sleep rhythms
b. Amount of sleep
B
Sleep rhythm power
Free-running period (h)
C
Sleep/circadian cycle (h)
Free-running period (h)
D
Model values
Experimental values
Power of experimental flies
Normalized power of simulated flies
Free–running period (h)
E
Model values
Experimental values
Sleep/circadian cycle (h)
Free–running period (h)

Figure 4

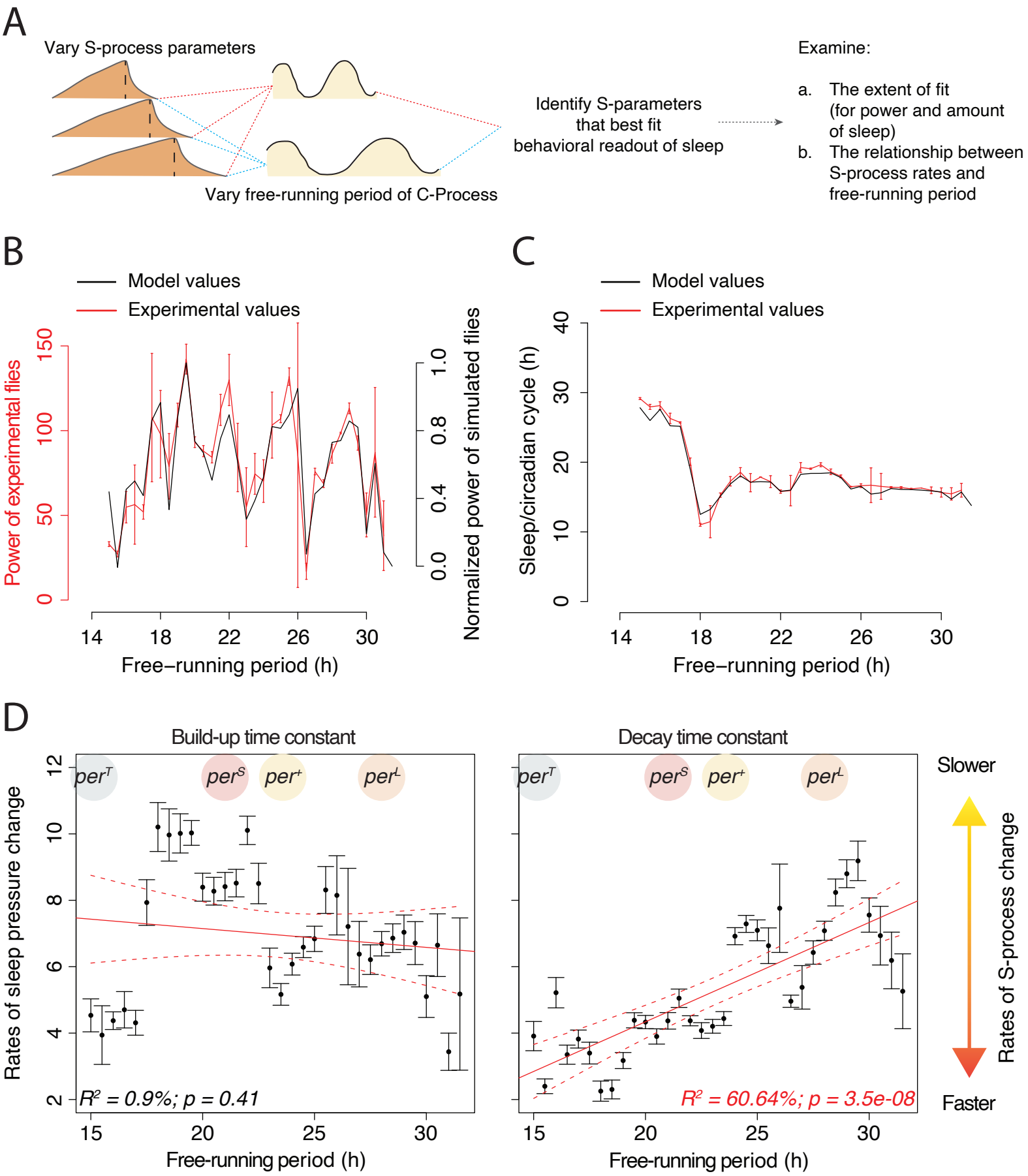
A
Vary S-process parameters
Vary free-running period of C-Process
Identify S-parameters that best fit behavioral readout of sleep
Examine:
a. The extent of fit (for power and amount of sleep)
b. The relationship between S-process rates and free-running period
B
Model values
Experimental values
Power of experimental flies
Normalized power of simulated flies
Free–running period (h)
C
Model values
Experimental values
Sleep/circadian cycle (h)
Free–running period (h)
D
Build-up time constant
Decay time constant
perT
perS
per+
perL
Rates of sleep pressure change
Free-running period (h)
R² = 0.9%; p = 0.41
R² = 60.64%; p = 3.5e-08
Slower
Faster
Rates of S-process change

Figure 5

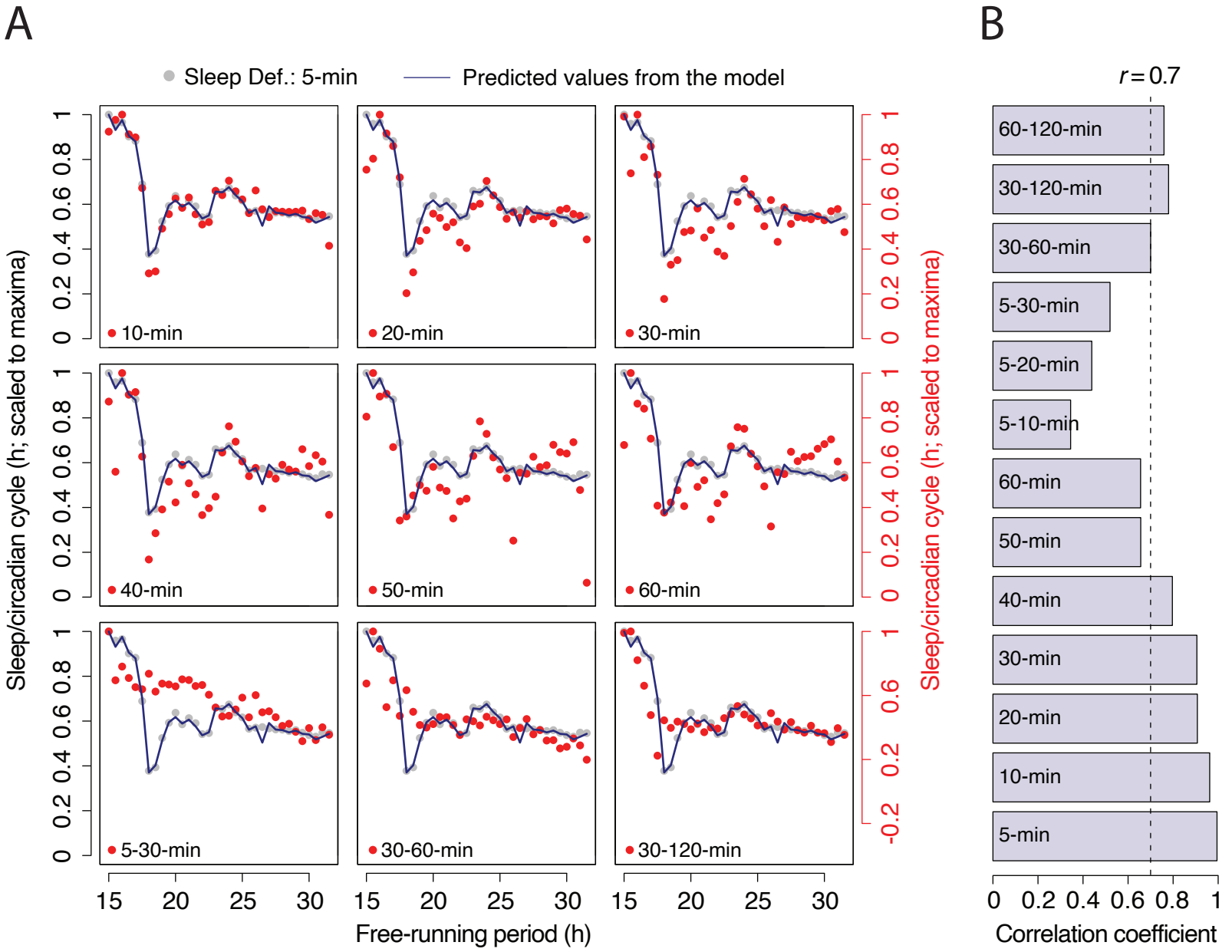
A
Sleep Def.: 5-min
Predicted values from the model
10-min
20-min
30-min
40-min
50-min
60-min
5-30-min
30-60-min
30-120-min
Sleep/circadian cycle (h; scaled to maxima)
Free-running period (h)
B
r = 0.7
60-120-min
30-120-min
30-60-min
5-30-min
5-20-min
5-10-min
60-min
50-min
40-min
30-min
20-min
10-min
5-min
Correlation coefficient

Figure 6

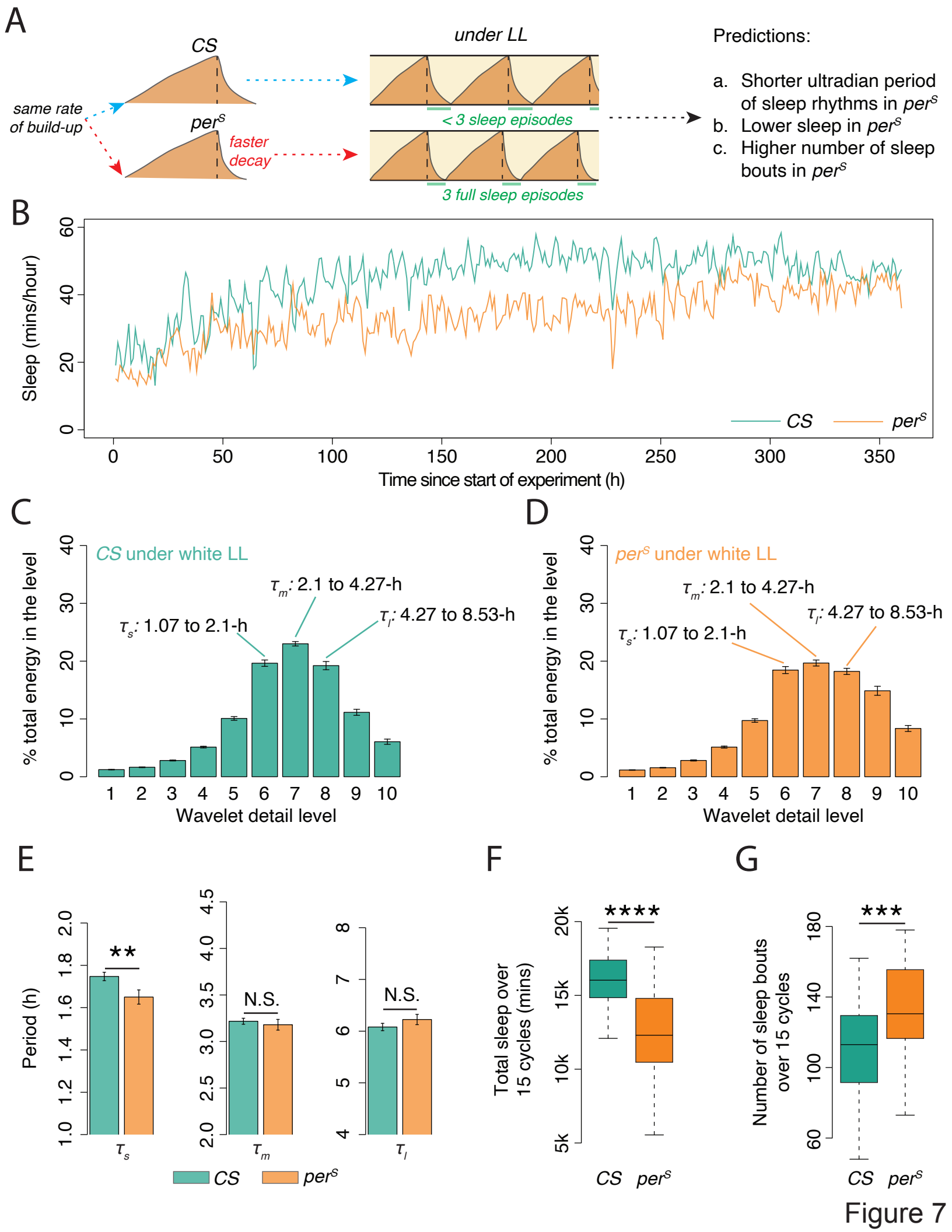
A
CS
per^S
same rate of build-up
faster decay
under LL
< 3 sleep episodes
3 full sleep episodes
Predictions:
a. Shorter ultradian period of sleep rhythms in per^S
b. Lower sleep in per^S
c. Higher number of sleep bouts in per^S
B
Sleep (mins/hour)
Time since start of experiment (h)
CS
per^S
C
CS under white LL
% total energy in the level
Wavelet detail level
τs: 1.07 to 2.1-h
τm: 2.1 to 4.27-h
τl: 4.27 to 8.53-h
D
per^S under white LL
% total energy in the level
Wavelet detail level
τs: 1.07 to 2.1-h
τm: 2.1 to 4.27-h
τl: 4.27 to 8.53-h
E
Period (h)
**
N.S.
N.S.
τs
τm
τl
CS
per^S
F
Total sleep over 15 cycles (mins)
****
CS
per^S
G
Number of sleep bouts over 15 cycles
***
CS
per^S

Figure 7

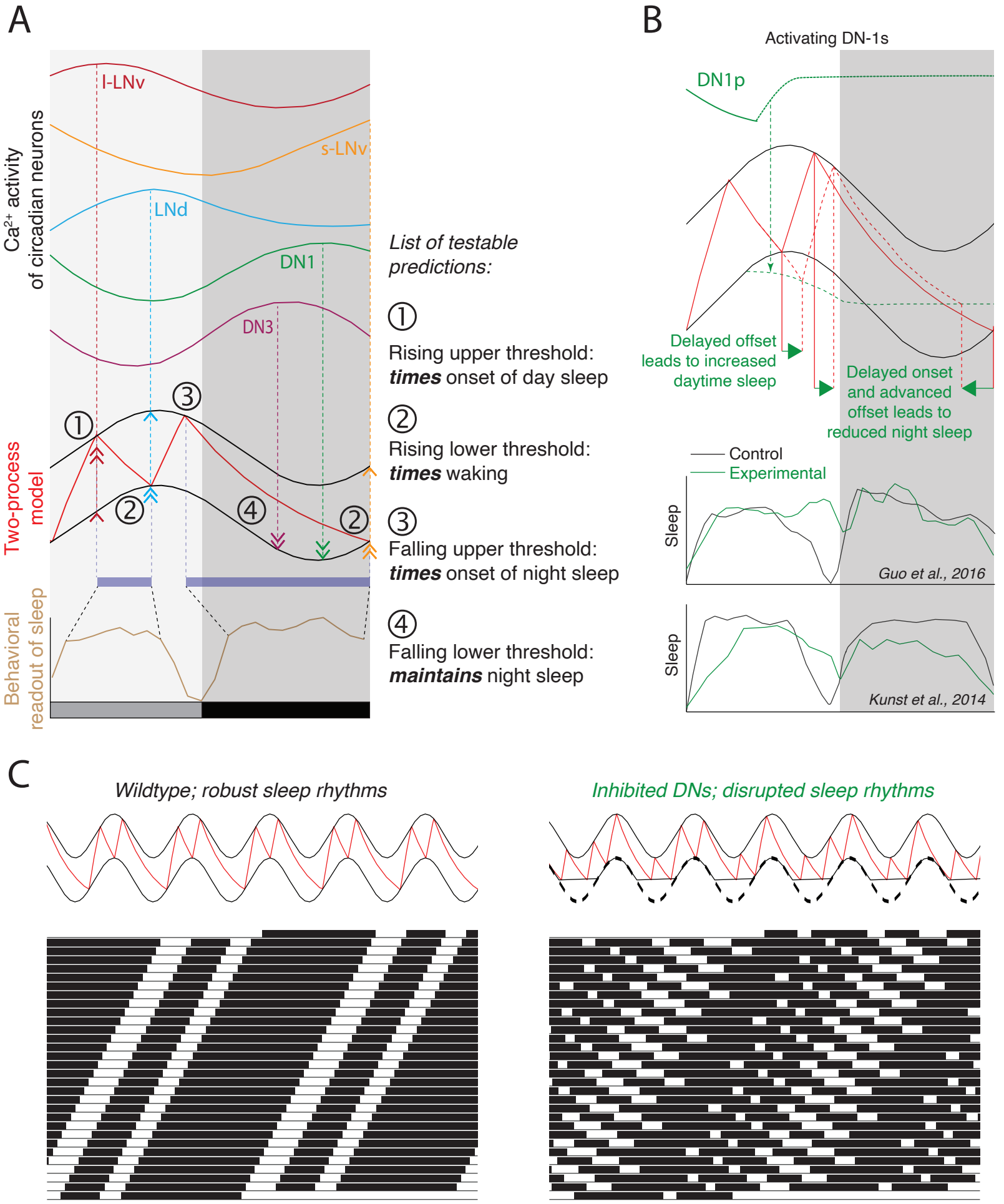
A
Ca2+ activity of circadian neurons
l-LNv
s-LNv
LNd
DN1
DN3
Two-process model
Behavioral readout of sleep
List of testable predictions:
① Rising upper threshold: times onset of day sleep
② Rising lower threshold: times waking
③ Falling upper threshold: times onset of night sleep
④ Falling lower threshold: maintains night sleep
B
Activating DN-1s
DN1p
Delayed offset leads to increased daytime sleep
Delayed onset and advanced offset leads to reduced night sleep
Control
Experimental
Sleep
Guo et al., 2016
Sleep
Kunst et al., 2014
C
Wildtype; robust sleep rhythms
Inhibited DNs; disrupted sleep rhythms

Figure 8